SAE The Engineering Resource For Advancing Mobility®

Gas Turbine Jet Exhaust Noise Prediction

SAENORM.COM : Click to view the full PDF of arp876c

ARP 876C

The Engineering Resource For Advancing Mobility®

400 COMMONWEALTH DRIVE, WARRENDALE, PA 15096

AEROSPACE RECOMMENDED PRACTICE

SAE ARP 876C

Issued 3-78
Revised 11-85

Superseding ARP 876B

Submitted for recognition as an American National Standard

GAS TURBINE JET EXHAUST NOISE PREDICTION

TABLE OF CONTENTS

SAENORM.COM : Click to view the full PDF of arp876c

SAE Technical Board Rules provide that: "This report is published by SAE to advance the state of technical and engineering sciences. The use of this report is entirely voluntary, and its applicability and suitability for any particular use, including any patent infringement arising therefrom, is the sole responsibility of the user."

SAE reviews each technical report at least every five years at which time it may be reaffirmed, revised, or cancelled. SAE invites your written comments and suggestions.

Copyright 1985 Society of Automotive Engineers, Inc.
All rights reserved.

Printed in U.S.A.

TABLE OF CONTENTS (Cont'd)

NOTE: The * Symbol is used in the margin to indicate changes of substance from the previous issue of this document.

PREPARED BY:

GAS TURBINE PROPULSION SUBCOMMITTEE OF
SAE COMMITTEE A-21, AIRCRAFT NOISE

SAENORM.COM : Click to view the full PDF of arp876c

1. INTRODUCTION

AIR 876, issued on 7 October 1965, presented a summary correlation of jet engine exhaust noise data available at that time. It dealt with both static and flight modes, but by virtue of the data largely being from full scale engines, no attempt was made to subdivide the information into the relevant component sources. Work in recent years on good-quality noise facilities has established that most engine exhaust systems are influenced in their noise characteristics by far more than the noise due to the external mixing process alone, and this work has provided the opportunity to develop a clearer picture of the influence of other effects.

AIR 876 was also limited to jet velocities above 1,000 ft/s, i.e. the range of exhaust velocities associated with early jet engines. The introduction of more advanced engine designs demands a prediction technique for exhaust sources over a far wider range of velocity conditions.

Therefore it is intended that ARP 876 be developed on a long term basis as a document definitive in most aspects of the prediction of exhaust noise, consistent with the state of the art. Specific recommended procedures will be issued as Appendices, both for completeness and to allow for future updating. Additionally, following a decision in 1979, explanatory background material detailing the rationale behind the selection of Appendix methods will be included in an Addendum to this document. The format of the Addenda will echo the main document for ease of cross reference.

The document will offer a method of estimating the exhaust noise from single unsilenced engines. To be useful in estimating the noise from aircraft installations, a number of additional effects must be considered, and it is intended that these also will be covered as substantive evidence becomes available.

Areas that will not be addressed in this ARP, due to source variability with detailed engine design parameters, are aerodynamic blade noise sources; that is the noise generated by interaction effects between rotating and stationary components of the fan, compressor and turbine systems.

Each Appendix will be dated, and will represent an approach to a particular topic as agreed by members of the SAE A-21 Subcommittee with experience or data on that subject. Lists of members and affiliated bodies contributing experimental data or other information as used in compiling any one Appendix will be included. Correspondence should be addressed to the Secretary of the A-21 Committee for appropriate distribution.

SAENORM.COM : Click to view the full PDF of arp876c

2. SOURCES OF EXHAUST NOISE

The exhaust system noise of gas turbine engines for aircraft applications can be considered to comprise the following main sources:

a) Pure jet mixing noise resulting from a hot core exhaust stream mixing with its surrounding environment (which may be influenced by a bypass flow).

b) Pure jet mixing noise resulting from a cold bypass stream mixing with both the surrounding environment and the core flow.

c) Shock associated noise, where either or both hot and cold exhaust systems comprise a choked final nozzle.

d) Noise from the core engine resulting from aerodynamic disturbances upstream of or at the final nozzle, including combustion noise.

e) Aerodynamic noise, tonal and broadband, resulting from blade interaction effects in fan, compressor or turbine systems.

All the above sources combine in varying degrees to produce the overall exhaust noise characteristics. The relevance of each source is a function of both engine operating condition and aircraft speed. Because of the dependence of aerodynamic blading noise on the intimate design configuration of any given engine, this aspect is specifically excluded from subsequent consideration, and every attempt has been made to remove such phenomena from any engine data used.

3. NOTES ON USE OF PREDICTION PROCEDURES

3.1 Prediction methods included in this document are self-contained. To develop an estimate of the total exhaust noise signature from an engine it is necessary to integrate the individual source components.

This is effected by estimating each component spectrum and summing the squared sound pressure levels in each one-third octave band. This is usually most conveniently carried out prior to any extrapolation to the relevant distance or corrections for atmospheric conditions and ground reflection effects. It is also necessary to incorporate any estimated turbo-machinery content (not covered herein) at the initial stage, in order to obtain a complete spectrum of engine noise. Furthermore, it is advisable that any assumed modification to the noise by virtue of silencing or installation effects is made in the component calculation stage.

SAENORM.COM : Click to view the full PDF of arp876c

3.2 Methods contained in this document are expressed in terms of noise levels that would be measured under free field conditions. Reflective augmentations and cancellations from real surfaces, primarily the ground surface over which measurements are made, produce peaks and troughs in the observed test spectra, and these have been corrected out of the experimental data used where it has not been obtained under anechoic conditions.

Spectra and directivity plots in this document must, therefore, be converted to non free-field conditions to make them representative of typical measurements "in the field". SAE AIR 1327 provides guidance on such conversion for an acoustically hard surface (i.e. concrete, tarmac) and advice on how to deal with other typical surfaces (e.g. grassland).

3.3 The prediction methods provide spectral information derived from measurements taken in the acoustic far field, but corrected for atmospheric attenuation and normalised for distance.

Since practical distances involved in aircraft noise calculations are large, apart from the normal inverse square law correction, allowance must be made for atmospheric absorption. SAE ARP 866A provides a standard method of allowing for atmospheric absorption under a range of ambient temperatures and humidity conditions.

3.4 If a subjective assessment is required, Perceived Noise Level (PNL) may be calculated using the methods in SAE ARP 865.

3.5 Prediction methods are directed at producing estimates of noise levels generated during the normal take-off and approach regimes of aircraft operation. Extrapolation of the methods to higher flight speeds, or use for estimation other than in the acoustic farfield, is not recommended since experimental evidence in support of such extrapolation was not available at the time of preparation of this document.

SAENORM.COM : Click to view the full PDF of arp876c

4. SYMBOLS

a	Speed of sound (at the local temperature)	m/s
a_o	Ambient speed of sound	m/s
A_j	Cross-sectional area of jet exhaust nozzle	m^2
C_v	Velocity coefficient for relevant discharge nozzle	
dB	Sound Pressure Level (re 20 Micro Pa.)	dB
DI	Farfield directivity index	dB
D_j	Exhaust nozzle diameter	m
f	One-third octave-band centre frequency	Hz
g	Gravitational constant	m/s^2
ISA	International Standard Atmosphere	
$\dot{M}$	Combustor mass flow rate	kg/s
$m(\theta_i)$	Relative Velocity exponent used in converting static mixing noise to flight conditions	
M_a	Aircraft flight Mach number (V_a/a_o)	
NPR	Nozzle pressure ratio	
OAPWL	Overall sound power level (re 1 pW)	dB
OASPL	Overall sound pressure level	dB
p	Static pressure	Pa
p_o	Ambient static pressure	Pa
p_{ISA}	Static pressure under ISA, SL conditions	Pa
P	Total pressure	Pa
P_o	Ambient-total pressure	Pa
P_{ISA}	Total pressure under ISA, SL conditions	Pa
Pref	Acoustical Reference Pressure, 20 μPa	Pa
PWL	One-third octave-band power level (re 1 pW)	dB

SAENORM.COM : Click to view the full PDF of arp876c

r	Radial distance from nozzle exit to observer	m
R	Gas constant with value 287.05 J/kg K based on the universal gas constant of 8.31432×10^3 J/[K(kg-mol)] and mass per kilogram-mole in dry air of 28.9644 kg/(kg-mol)	J/kg K
S	Normalised free-field Overall Sound Pressure Level	dB
S(f)	Power level spectrum shape factor	dB
SPL	Sound pressure level (re 20 μPa)	dB
t	Static temperature	K
t_o	Ambient static temperature	K
T	Total temperature	K
T_o	Ambient total temperature	K
T_j	Jet total temperature	K
V_a	Forward speed of engine (i.e. airplane)	m/s
V_j	Fully expanded jet velocity	m/s
π_{ref}	Acoustical reference power, 1 pW	watt
	Ratio of specific heats for propulsive medium	
θ_i	Angle to engine intake axis	degrees
θ_j	Angle to engine jet axis ($180^\circ - \theta_i$)	degrees
ρ	Density	kg/m^3
ρ_{ISA}	Atmospheric density under ISA conditions (1.225 kg/m^3 based on atmospheric pressure of 1.01325×10^5 Pa at an air temperature of 288.15 K)	kg/m^3
ρ_j	Fully expanded jet density	kg/m^3
ω	Variable density index used in computing OASPL from jet mixing noise	
ϕ	Angle between direction of aircraft motion and direction of sound propagation	degrees

SAENORM.COM : Click to view the full PDF of arp876c

ψ	Angle between airplane flight path and engine thrust axis	degrees
ξ	Strouhal frequency adjustment factor	

NOTE: The units quoted above for the physical quantities are the recommended Systeme Internationale units. Except for the logarithmic quantities, temperatures and angles, any other consistent system of units may be used since results are expressed as dimensionless ratios.

SAENORM.COM : Click to view the full PDF of arp876c

APPENDIX A

DATE OF COMPILATION
Static Conditions - September 1976
Flight Conditions - November 1978

5. PREDICTION OF SINGLE STREAM JET MIXING NOISE FROM SHOCK FREE CIRCULAR NOZZLES

5.1 Static Conditions: Definitive model scale experimental work in the 1970's provided a firm data base for the study of mixing noise over a wide range of jet velocity and temperature conditions. That work showed that jet mixing noise level and spectral character is a function of the following principal parameters:

a) The velocity differential between that of the jet and its environment.

b) The jet density relative to the density of the surrounding air.

c) The jet dimensions.

It has been concluded that one of the most convenient ways to express jet noise characteristics is to consider first the normalized overall sound pressure level (OASPL) as a function of jet velocity (V_j) and angle of measurement (θ_i or θ_j) and to then relate the spectrum (on a one-third octave-band basis) to the overall level at any point in the field. This procedure may be adopted by using Figs. A1 through A11. The information in Fig. A1 through Fig. A11 is also presented in Tables A1 through A11.

The method of calculation is as follows:

Step 1 - Calculate the fully expanded mean jet velocity (V_j) from a knowledge of jet temperature and pressure, where:

$$V_j = C_v \left\{ [(2\gamma Rg)/(\gamma - 1)][T_j][1 - NPR^{-(\gamma - 1)/\gamma}] \right\}^{1/2}$$

or, where a knowledge of temperature and pressure is not readily available (for example, from engine test stand measurements) an alternative method of calculating V_j is from thrust and mass flow, where:

V_j = static gross thrust divided by mass flow

Step 2 - Using V_j obtained from Step 1 and the ambient speed of sound (a_o) obtain the variable density index (ω) from Fig. A1.

SAENORM.COM : Click to view the full PDF of arp876c

5.1 (Continued)

Step 3 - For any desired angle and jet velocity use Fig. A2 to obtain the normalized free-field overall sound pressure level (S) where:

$$S = OASPL - 10 \log_{10} \left\{ [(\rho_j/\rho_o)^{\omega}](A_j/r^2) \right\} - 20 \log_{10}(P_o/P_{ISA})$$

for the value of V_j at any desired angle.

Step 4 - Calculate the overall sound pressure level (OASPL) from:

$$OASPL = S + 10 \log_{10}(\rho_j/\rho_o)^{\omega} + 10 \log_{10} (A_j/r^2) + 20 \log_{10} (P_o/P_{ISA})$$

Step 5 - Calculate the one-third octave-band spectral levels from Figs. A3 to A11, using jet velocity (V_j), temperature ratio (T_j/T_o), nozzle diameter (D_j) and the angle (θ_i) as follows:

Determine the Strouhal frequency adjustment factor from Fig. A3 and then calculate ($fD_j/\xi V_j$) for each one-third octave-band centre frequency. Enter Figs. A4 to A11 with the values of ($fD_j/\xi V_j$), and values of (T_j/T_o) at the values of $\log_{10}$ (V_j/a) and θ_i to determine values of one-third octave-band relative sound pressure level (SPL - OASPL).

For values other than those specified in Figs. A3 - A11, linear interpolation on angles (θ_i), and on the values for $\log_{10}$ ($fD_j/\xi V_j$), $\log_{10}$ (V_j/a_o) and (T_j/T_o) is recommended.

Step 6 - From the values of OASPL and one-third octave-band relative sound pressure level (SPL - OASPL) as derived in steps 4 and 5 respectively, calculate values of one-third octave-band SPL.

These values represent the free-field jet noise spectrum at position (r, θ_i) in a loss free atmosphere.

SAENORM.COM : Click to view the full PDF of arp876c

Note 1 The spectra of Figs. A3 - A11 satisfy the following condition

$$\log_{10} \left[\sum_{i=1}^{N} 10^{0.1(SPL_i - OASPL)} \right] = 0$$

Over the range of one-third octave-band frequencies defined by

$$-1.6 \leq \log_{10} (fD_j/\xi V_j) \leq 1.6$$

5.1 (Continued)

Note 2 Accuracy of Prediction

The accuracy of prediction of OASPL at (r, θ_i) relative to the model data on which it is based varies between ±2 dB at low jet velocities to ±4 dB at very high jet velocities. The accuracy of prediction of one-third octave (SPL- OASPL) varies between ±1 dB at frequencies near the peak of the jet-noise spectrum. However, these limits apply to the extreme cases. For all normal purposes, the majority of predictions will be accurate within ±3 dB at all frequencies.

Note 3 For the derivation and substantiation of the method, references may be made to the following documents:

(i) Boeing Document No. D6 - 42929 - 1, Empirical Jet Noise Predictions for Single and Dual Flow Jets and without Suppressor Nozzles Volume 1. Single flow Subsonic and Supersonic Jets. C. L. Jaeck, S. J. Cowan, R. P. Gerend.

(ii) SNECMA Document YKA No. 5898/76, Comparison des spectres 1/3 d'octave de bruit de jet mesures en chambre sourde A 17 de CEPr aux diverses propositions de revision de l'ARP 876 de la SAE.

(iii) SNECMA Document YKA No. 5317/75, Revision de la methode de prevision du bruit des jets (SAE ARP 876).

5.2 Flight Condition:

Forward speed has the effect of reducing the shear between the jet and its environment. Work in the 1970's produced conflicting evidence on the change in jet mixing noise in going from static to flight conditions. Model scale wind tunnel testing has, in general, produced a greater reduction in level than tests carried out on ground based engine facilities and aircraft. The differences may be associated with contamination by other sources, both engine based and aircraft installation induced. The method herein is based upon data obtained on a ground based engine flight simulation facility.* In general, the results of applying the prediction method fall between the extremes represented by some model tests and some aircraft flight tests.

The method relies upon a modification of the static sound pressure levels obtained in 5.1.

*For a description of the facility on which much of the basic data used herein were acquired, reference may be made to the AIAA Paper No. 76-534, July 1976, entitled, "Use of the Bertin Aerotrain for the Investigation of Flight Effects on Aircraft Engine Exhaust Noise," by R. G. Hoch and M. Berthelot.

SAENORM.COM : Click to view the full PDF of arp876c

5.2 (Continued)

For a jet of given velocity V_j (corresponding to a given pressure ratio and temperature), moving at a flight speed V_a, the method of calculation is as follows:

Step 1 - Calculate the free field static overall sound pressure levels (OASPL) as a function of angle to inlet axis, as outlined in steps 1 to 4 of 5.1, corresponding to the exhaust conditions.

Step 2 - Calculate the OASPL in flight at any desired angle θ_i ($20^\circ \leq \theta_i \leq 160^\circ$):

$$[OASPL(\theta_i)]_{flight} = [OASPL(\theta_i)]_{static} - \Delta OASPL(\theta_i)$$

where

$$\Delta OASPL(\theta_i) = 10 \log_{10}\left\{\left(\frac{V_J}{V_j - V_a}\right)^{m(\theta_i)} (1 - M_a \cos \phi)\right\}$$

with:

$m(\theta_i)$ = relative velocity exponent, a function of angle θ_i between the engine inlet axis and the line connecting an aircraft reference point * and the observer location; $m(\theta_i)$ is given in Fig. A12 and Table A12

$M_a = V_a/a_o$ = Aircraft flight Mach number or ratio of airspeed V_a to speed of sound a_o at the ambient temperature of the surrounding medium

ϕ = angle between direction of aircraft motion and direction of propagation (see sketch next page)

V_j = ideal fully expanded jet velocity, corresponding to a given pressure ratio and total temperature of the jet and being the same in static and in flight, see Eq. (A1)

NOTE: For consistency with the prediction procedure under static conditions, the aircraft reference point * should be the center of the nozzle exit. For practical applications (aircraft noise predictions) alternative reference points may have to be selected (e.g. center of the engine nacelle, or centroid of the nozzle exits for airplanes powered by more than one engine, etc.)

SAENORM.COM : Click to view the full PDF of arp876c

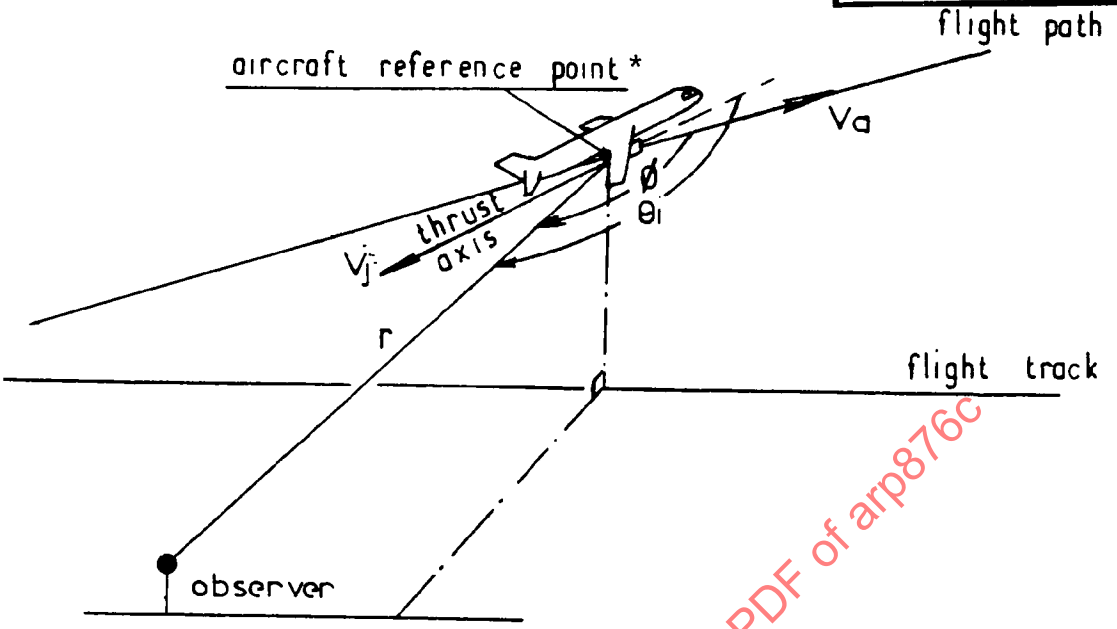

5.2 (Continued)

Step 3 - Calculate the one-third octave-band sound pressure levels in flight for any desired angle θ_i, following steps 5 and 6 of 5.1., with the exception that now the OASPL is the value in flight as derived in step 2 of this section and that the Strouhal number

$$(fD_j/\xi V_j)$$

has to be replaced by one based on relative jet velocity $(V_j - V_a)$, that is:

$$[fD_j/\xi(V_j - V_a)]$$

The value of ξ is still obtained from Fig. A3 for the corresponding value of the jet velocity V_j.

NOTE: Accuracy of Prediction

The accuracy of $\Delta OASPL(\theta_i)$ prediction, as calculated in step 2 for any angle θ_i, is a function of velocity ratio, and may be obtained from the following formula:

$$\pm\delta[\Delta OASPL(\theta_i)] = \pm[\delta m(\theta_i)] \times \left\{10 \log_{10}[V_j/(V_j - V_a)]\right\}$$

$\delta m(\theta_i)$ being the uncertainty in $m(\theta_i)$.

In the present prediction procedure, the range of uncertainty of the exponent $m(\theta_i)$ with respect to aircraft flight test data is estimated to not exceed ±one unit. This comment does not apply to wind tunnel model data where the exponent $m(\theta_i)$ is always greater, than ±one unit over the angular range $60^\circ \leq \theta i \leq 130^\circ$, and by as much as 0 to 5 units.

SAENORM.COM : Click to view the full PDF of arp876c

5.3 Parties Contributing to Formulation of Appendix A

Department of Transportation, USA
Douglas Aircraft Company, USA
General Electric Company, USA
Hamilton Standard, USA
Lockheed California Company, USA
Lockheed Georgia Company, USA
National Aeronautics Space Administration, USA
National Gas Turbine Establishment, United Kingdom
Pratt Whitney Aircraft Company, USA
Rolls-Royce Limited, United Kingdom
SNECMA, France
The Boeing Company, USA

SAENORM.COM : Click to view the full PDF of arp876c

Variable density index ω

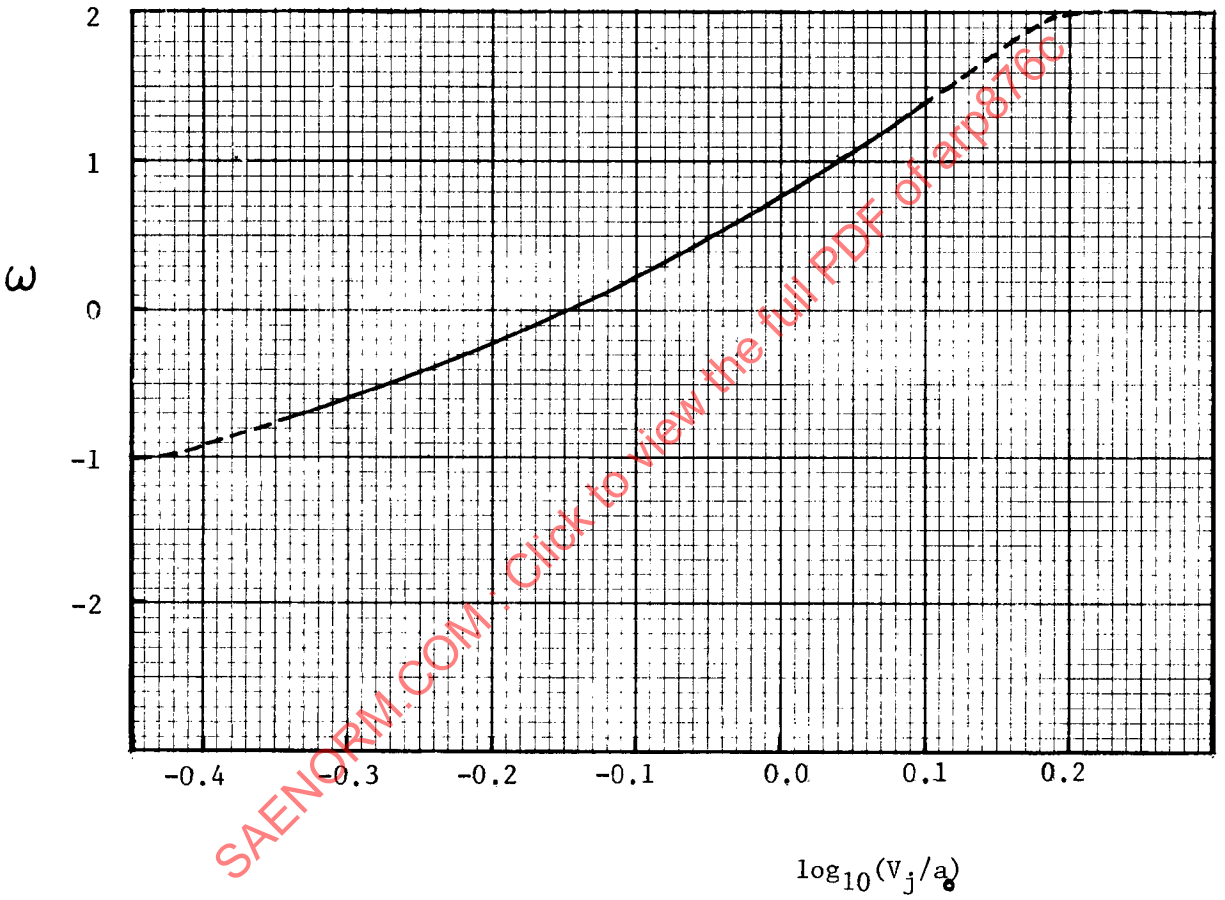

SAENORM.COM : Click to view the full PDF of arp876c

Note: Experimental evidence is represented by the solid line.

Above $\log_{10}(V_j/a_0) = 0.2$, the value of ω should be taken as 2.0

FIGURE A1

CARPET PLOT FOR NORMALIZED OVERALL SOUND
PRESSURE LEVELS OF PURE JET-MIXING NOISE

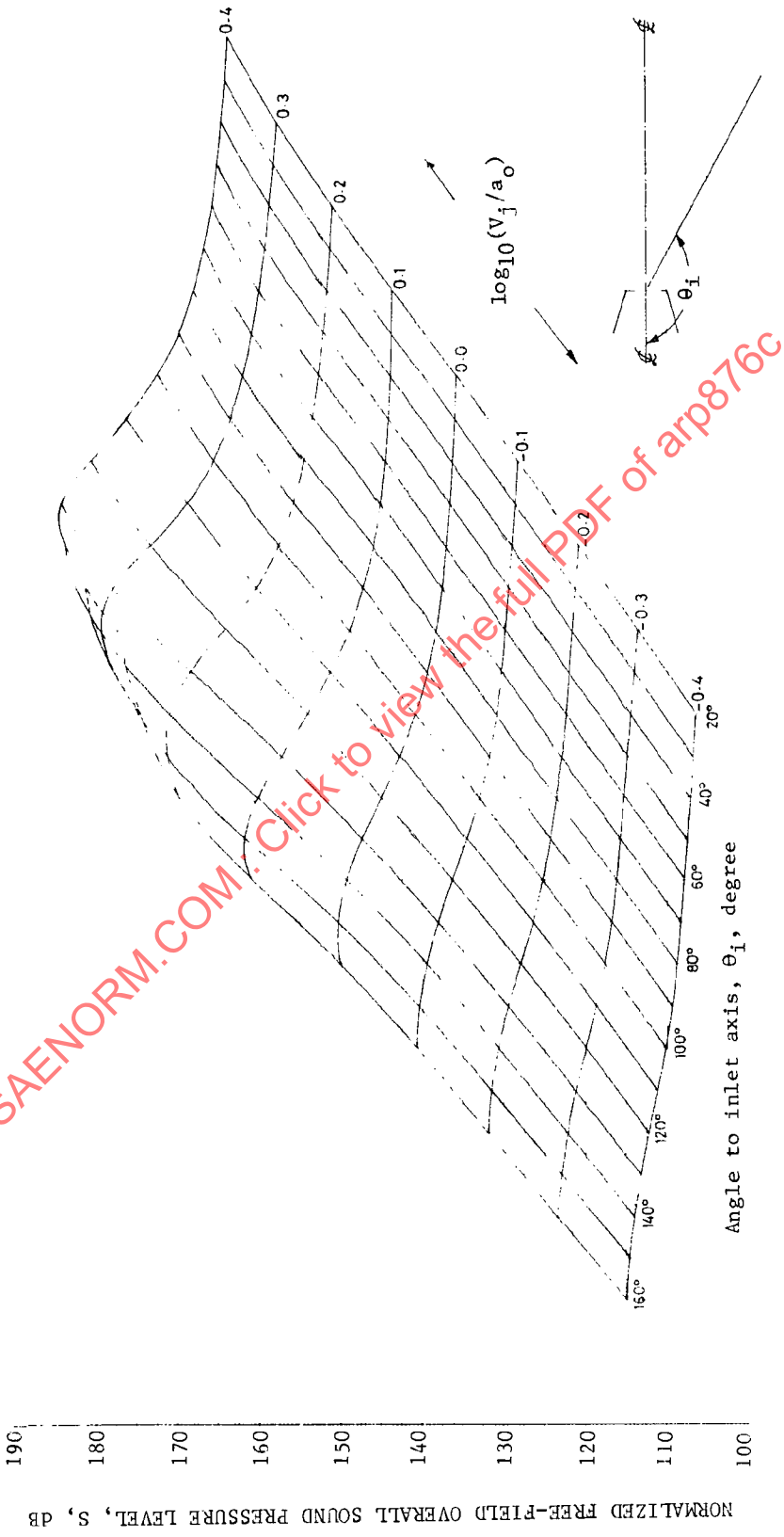

FIGURE A2

SAENORM.COM : Click to view the full PDF of arp876c

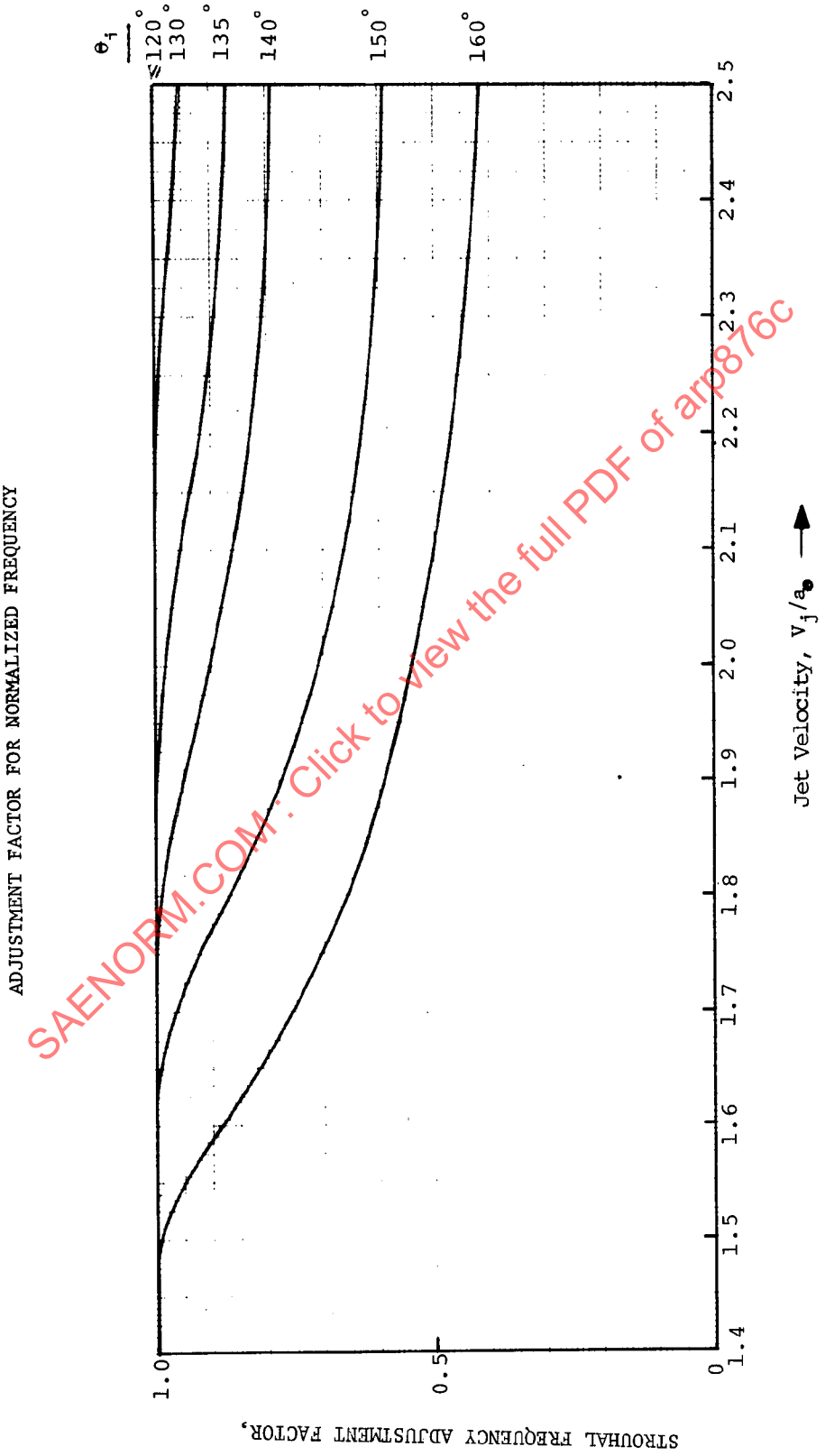

FIGURE A3

SAENORM.COM : Click to view the full PDF of arp876c

ONE-THIRD OCTAVE-BAND NORMALISED SPECTRA $\theta_i < 90°$

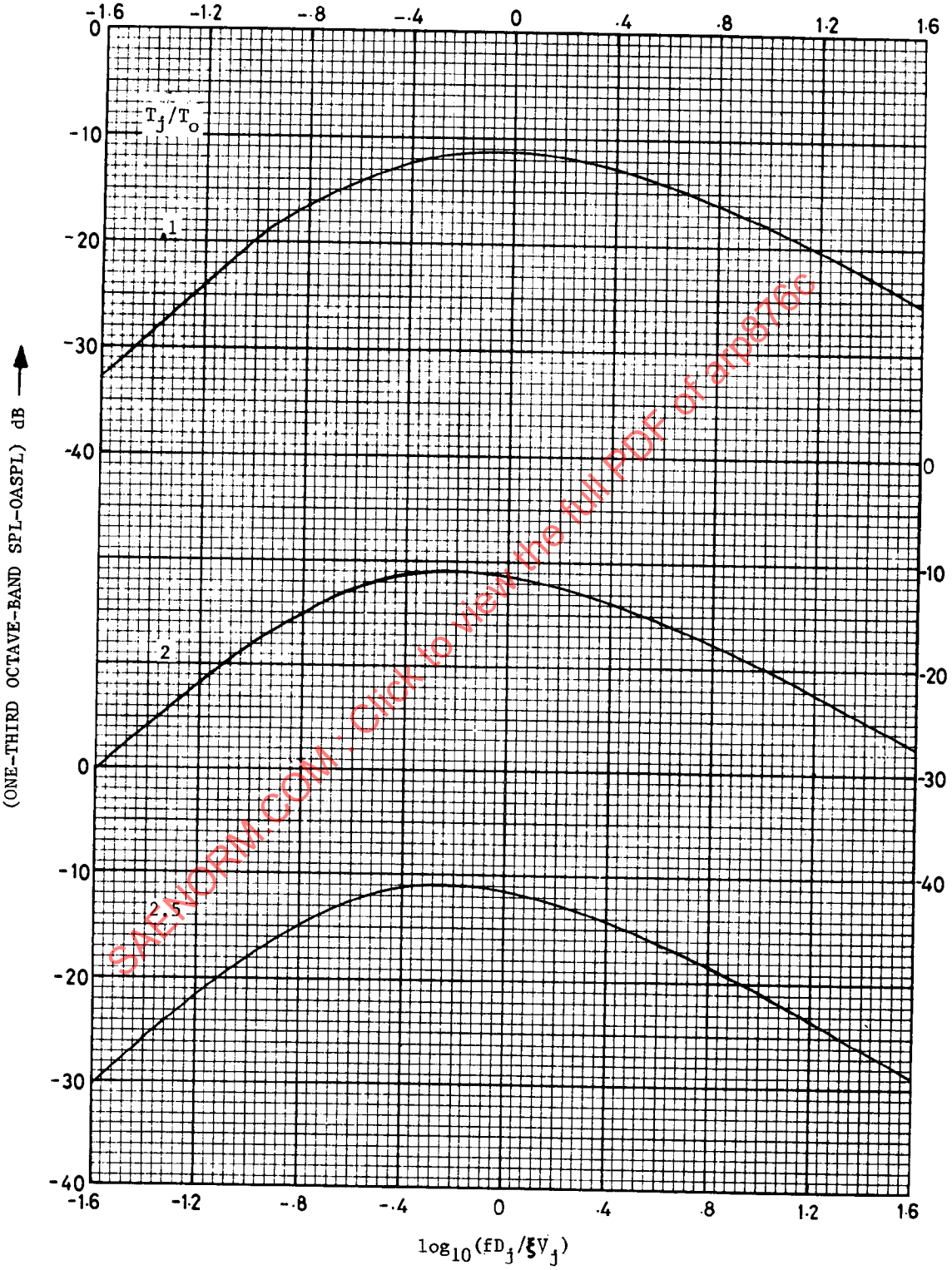

SAENORM.COM : Click to view the full PDF of arp876c

FIGURE A4

ONE-THIRD OCTAVE-BAND NORMALISED SPECTRA $\theta_i \leq 90°$

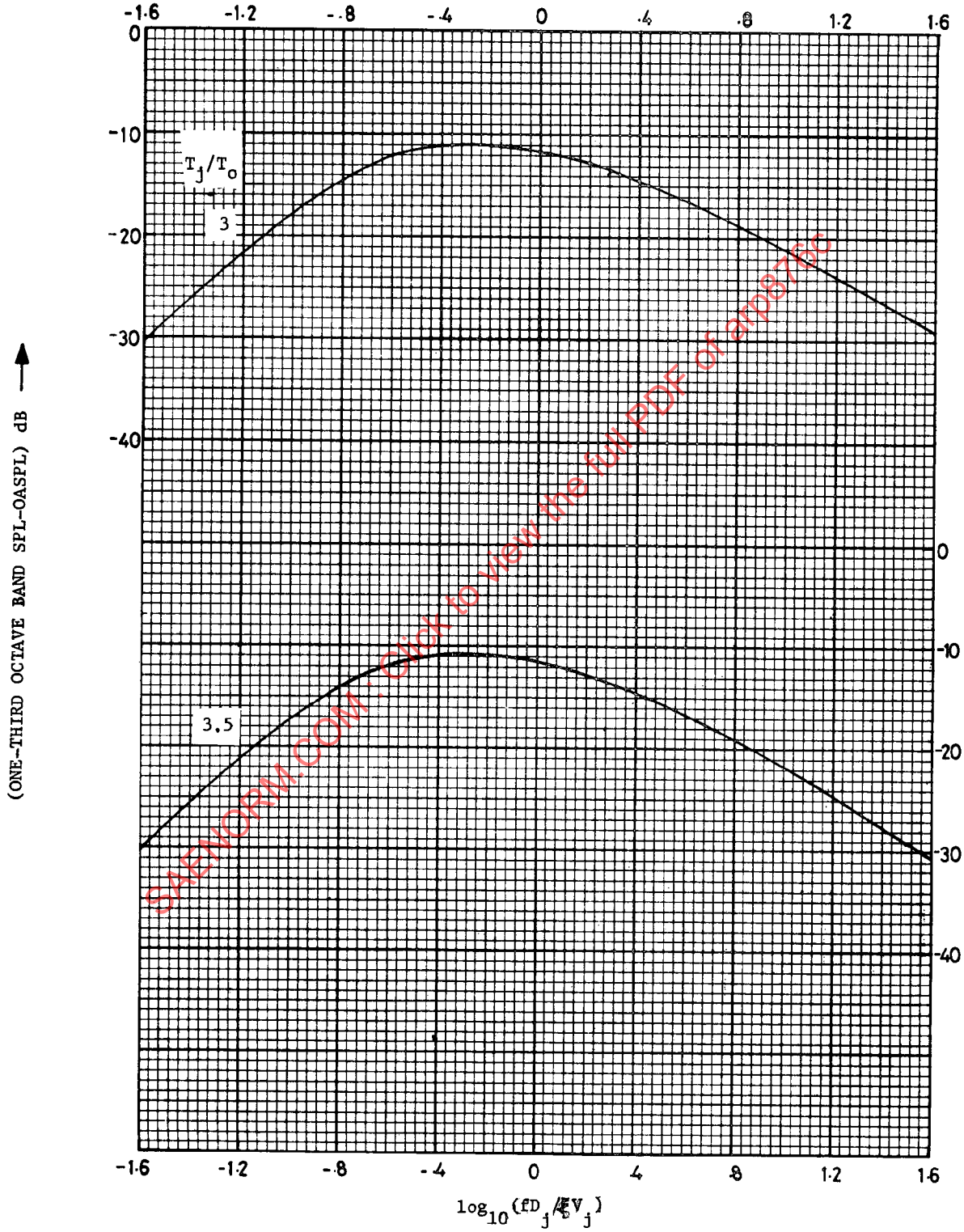

SAENORM.COM : Click to view the full PDF of arp876c

FIGURE A4 (CONT'D)

ONE-THIRD OCTAVE-BAND NORMALISED SPECTRA $\theta_i = 100°$

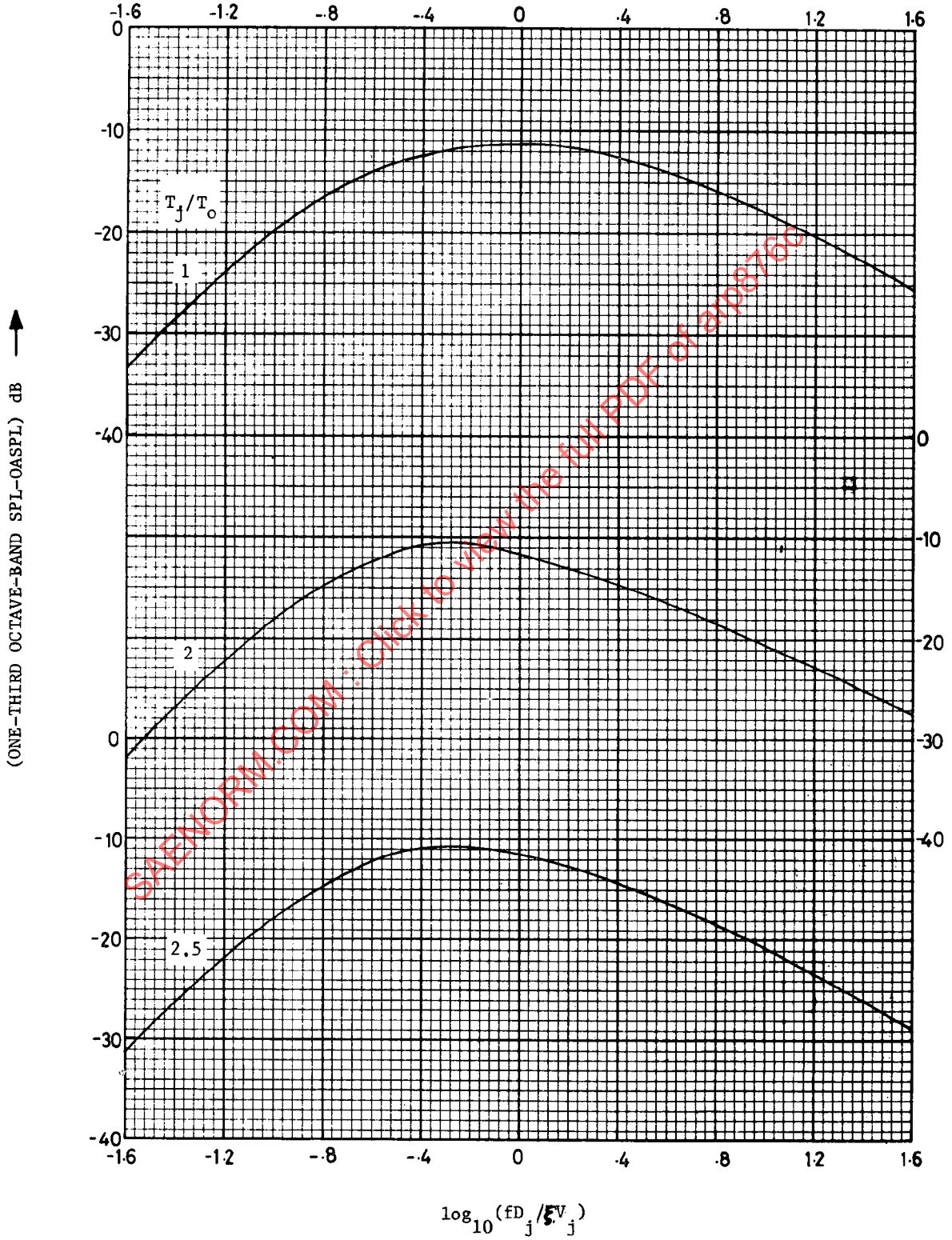

SAENORM.COM : Click to view the full PDF of arp876c

FIGURE A5

ONE-THIRD OCTAVE-BAND NORMALISED SPECTRA $\theta_i = 100°$

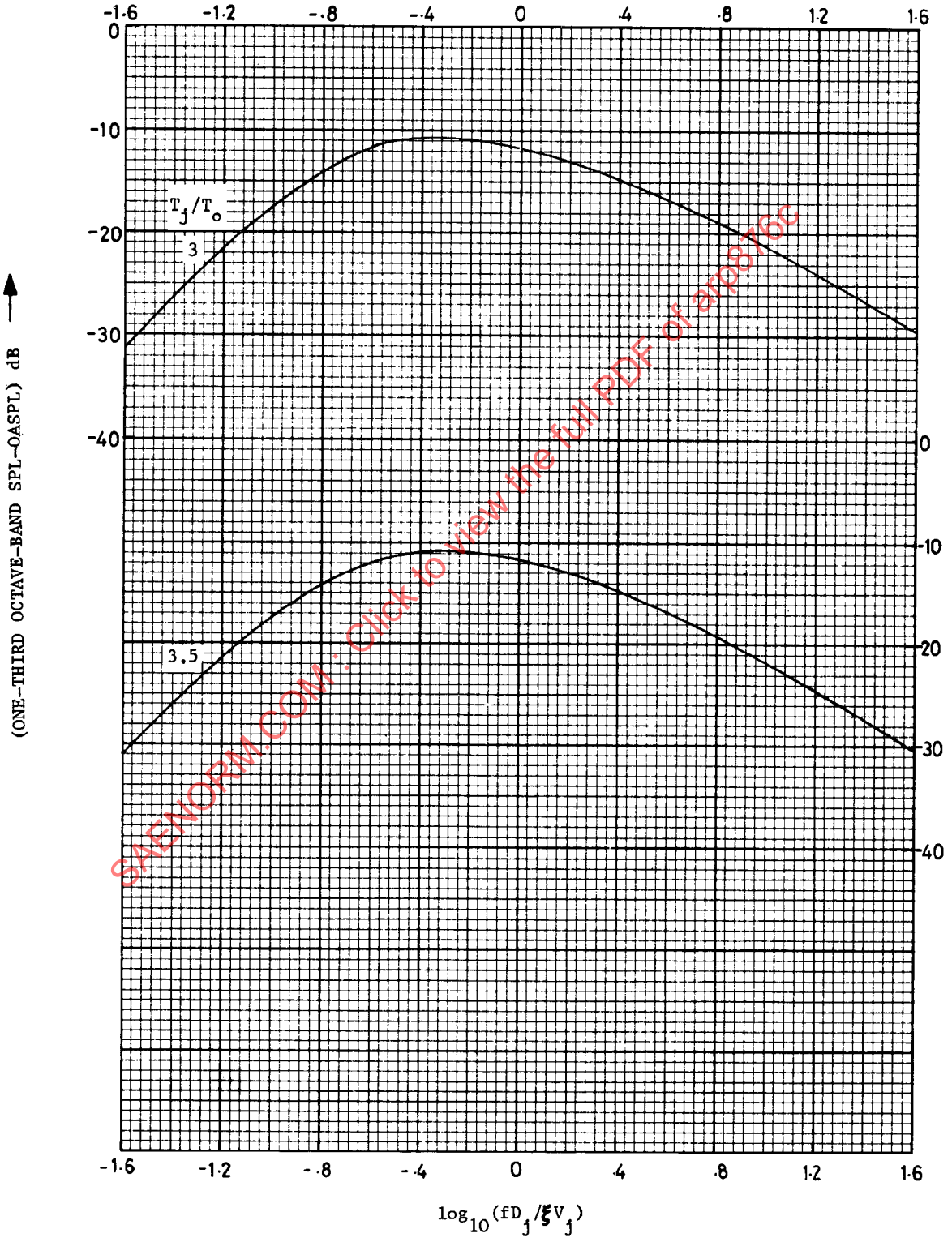

SAENORM.COM : Click to view the full PDF of arp876c

FIGURE A5 (CONT'D)

ONE-THIRD OCTAVE-BAND NORMALISED SPECTRA $\theta_i = 110°$

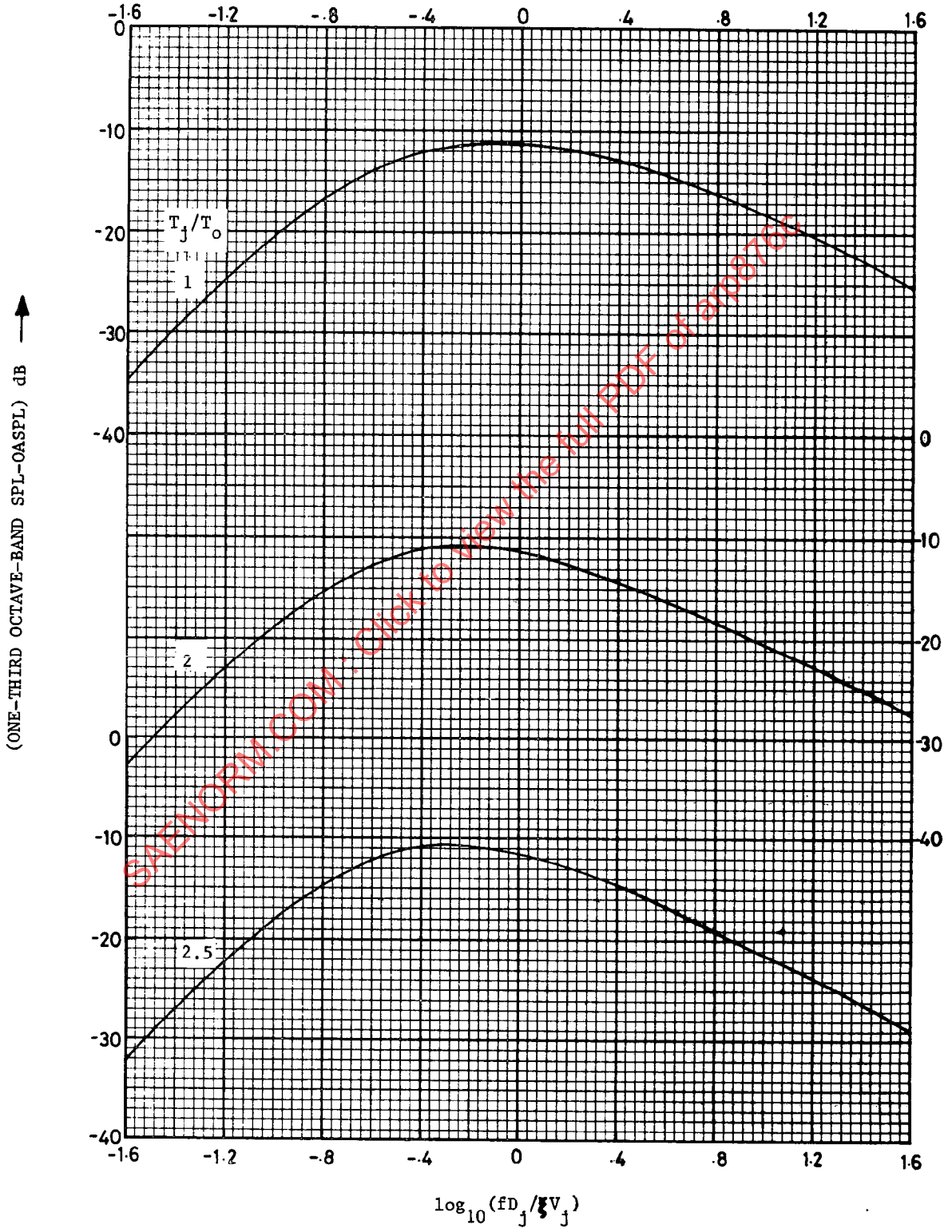

SAENORM.COM : Click to view the full PDF of arp876c

FIGURE A6

ONE-THIRD OCTAVE-BAND NORMALISED SPECTRA $\theta_i = 110°$

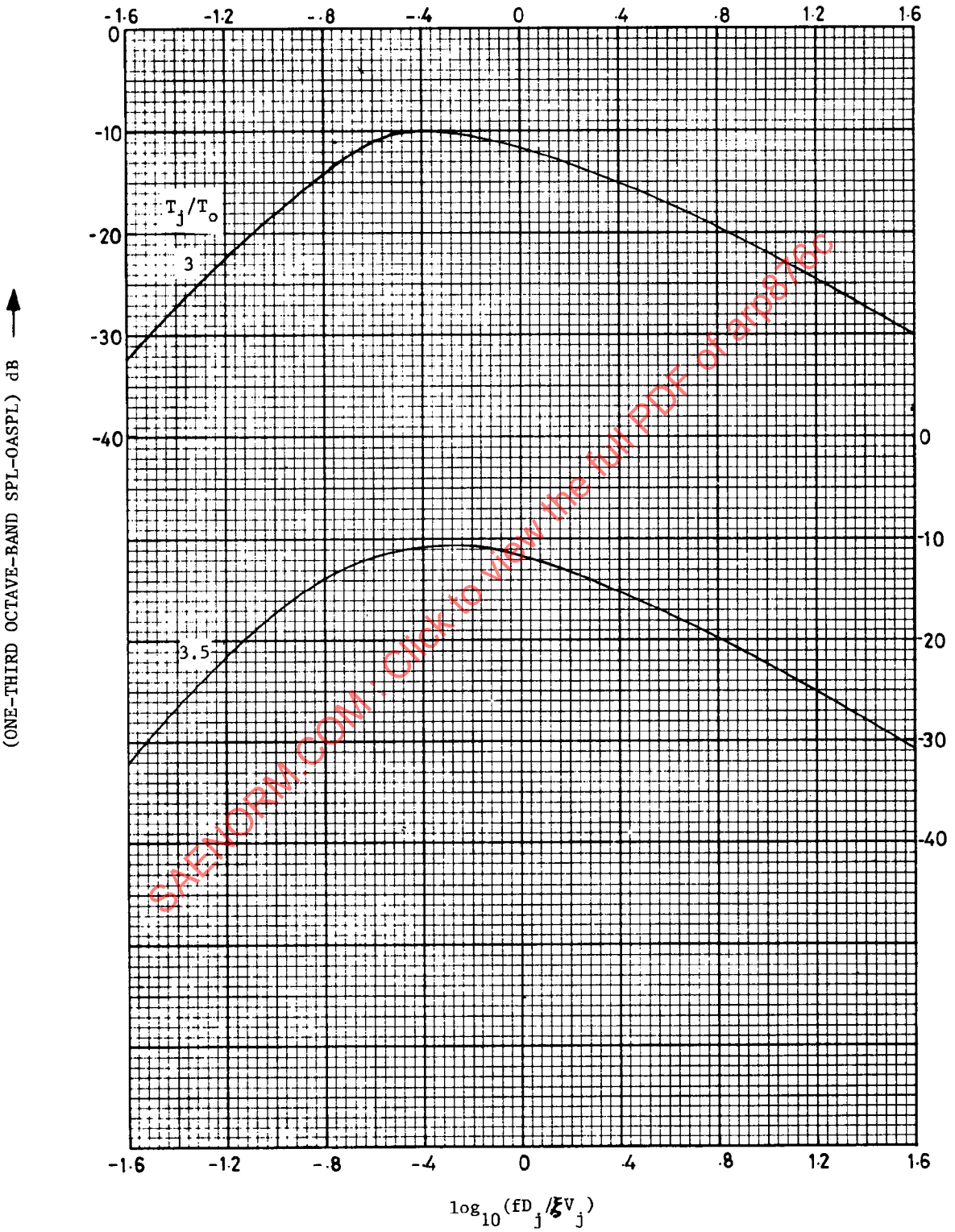

SAENORM.COM : Click to view the full PDF of arp876c

FIGURE A6 (CONT'd)

ONE-THIRD OCTAVE-BAND NORMALISED SPECTRA $\theta_i = 120°$

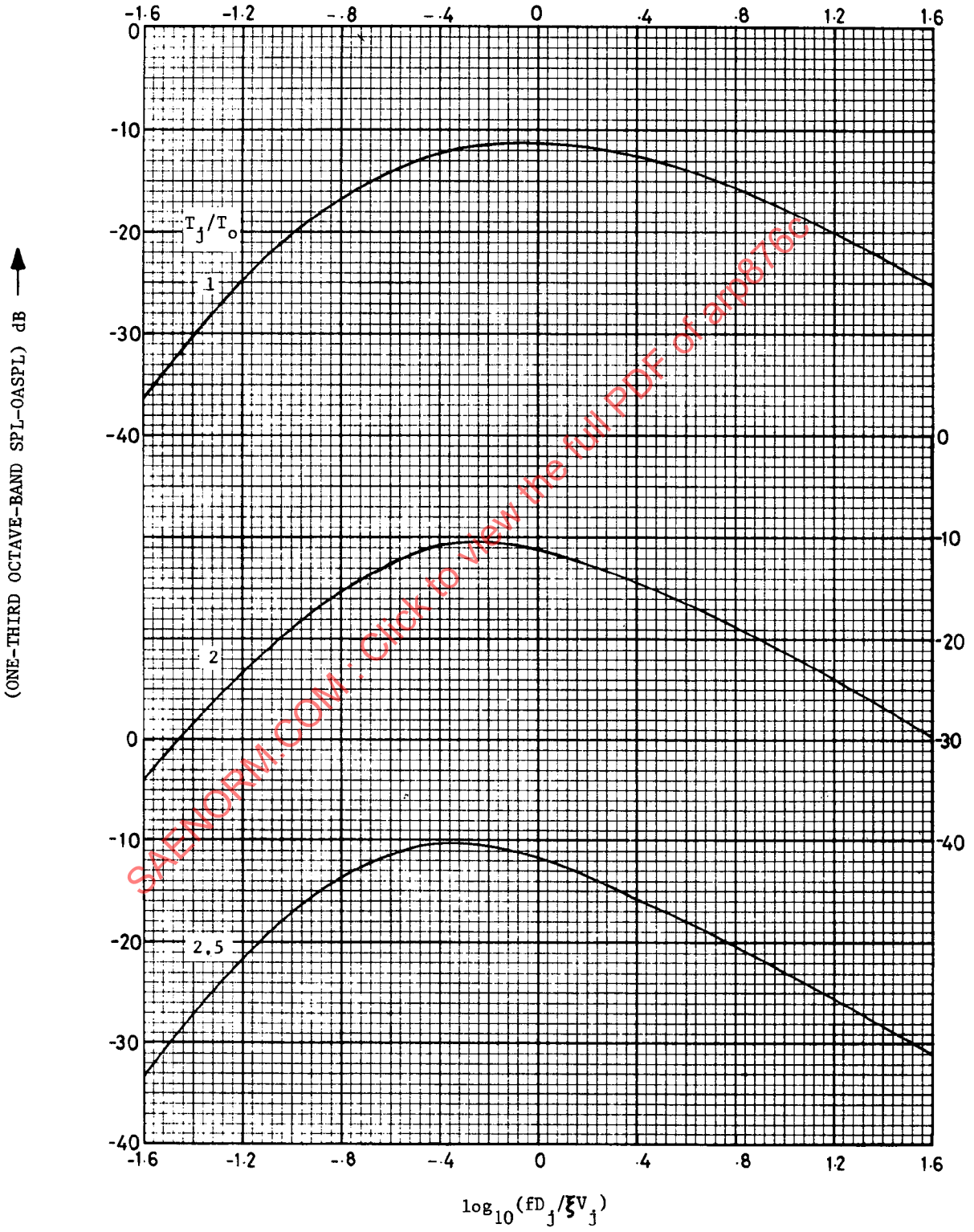

SAENORM.COM : Click to view the full PDF of arp876c

FIGURE A7

ONE-THIRD OCTAVE-BAND NORMALISED SPECTRA $\theta_i = 120°$

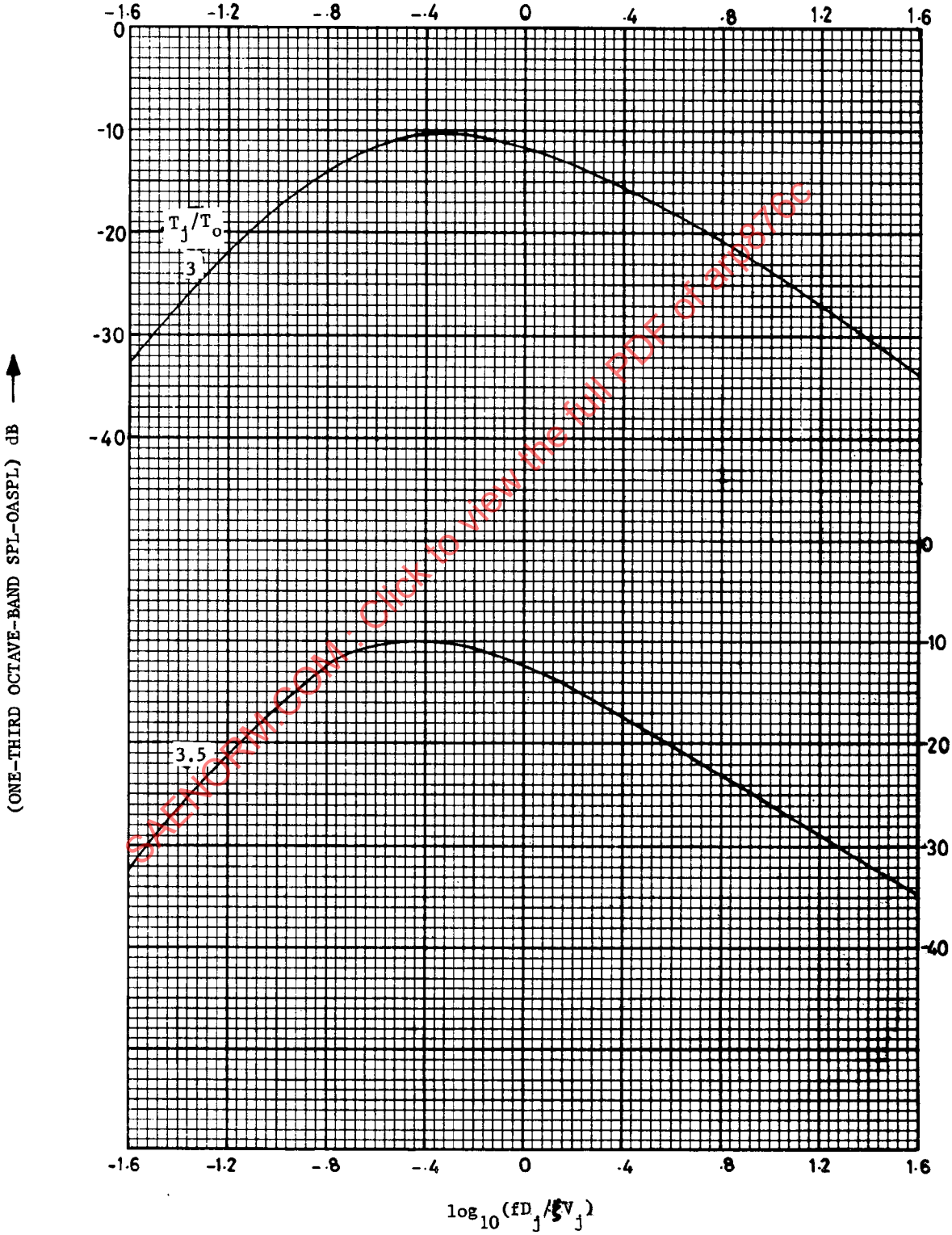

SAENORM.COM : Click to view the full PDF of arp876c

FIGURE A7 (CONT'D)

ONE-THIRD OCTAVE-BAND NORMALISED SPECTRA $\theta_i = 130°$.

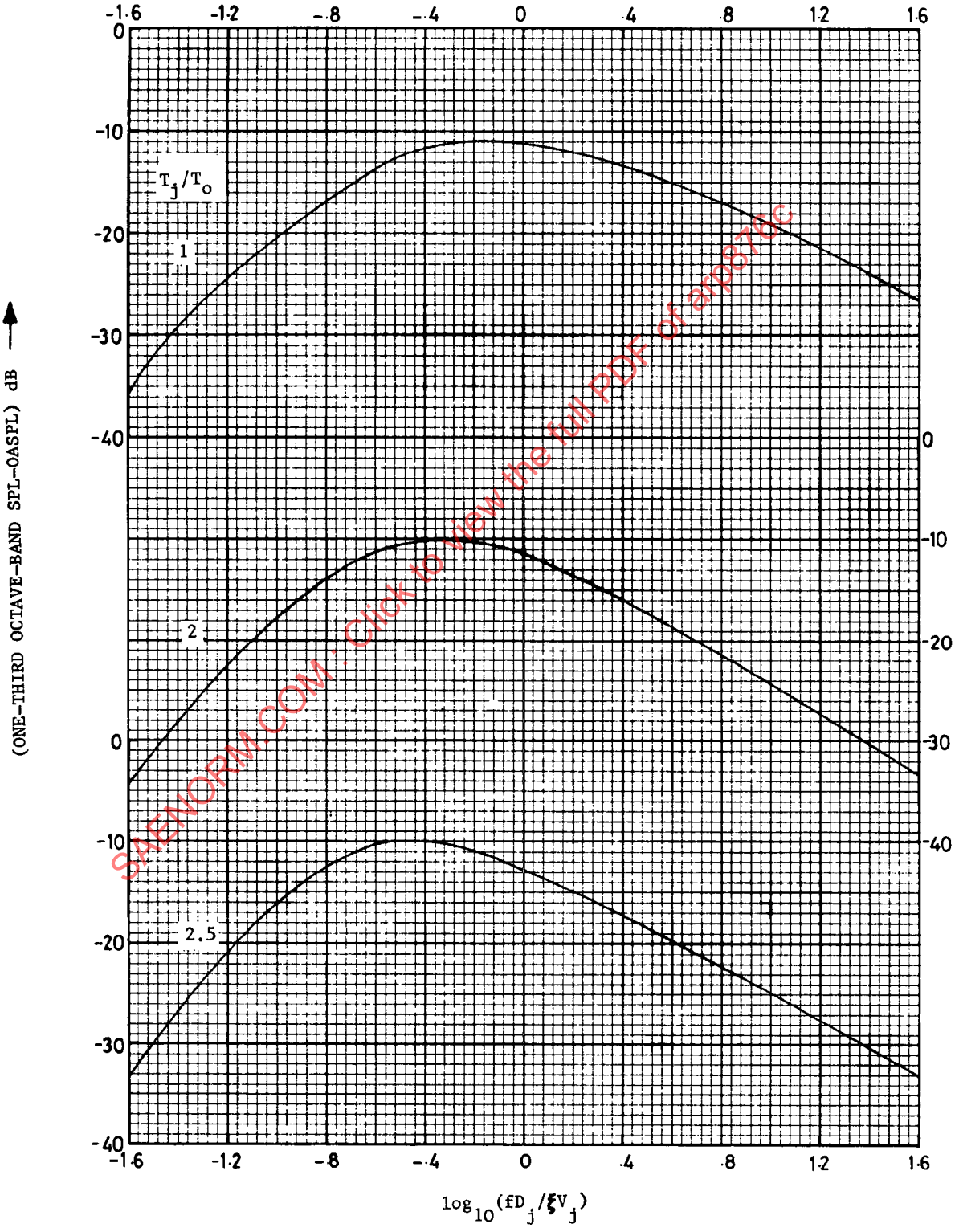

SAENORM.COM : Click to view the full PDF of arp876c

FIGURE A8

ONE-THIRD OCTAVE-BAND NORMALISED SPECTRA $\theta_i = 130°$

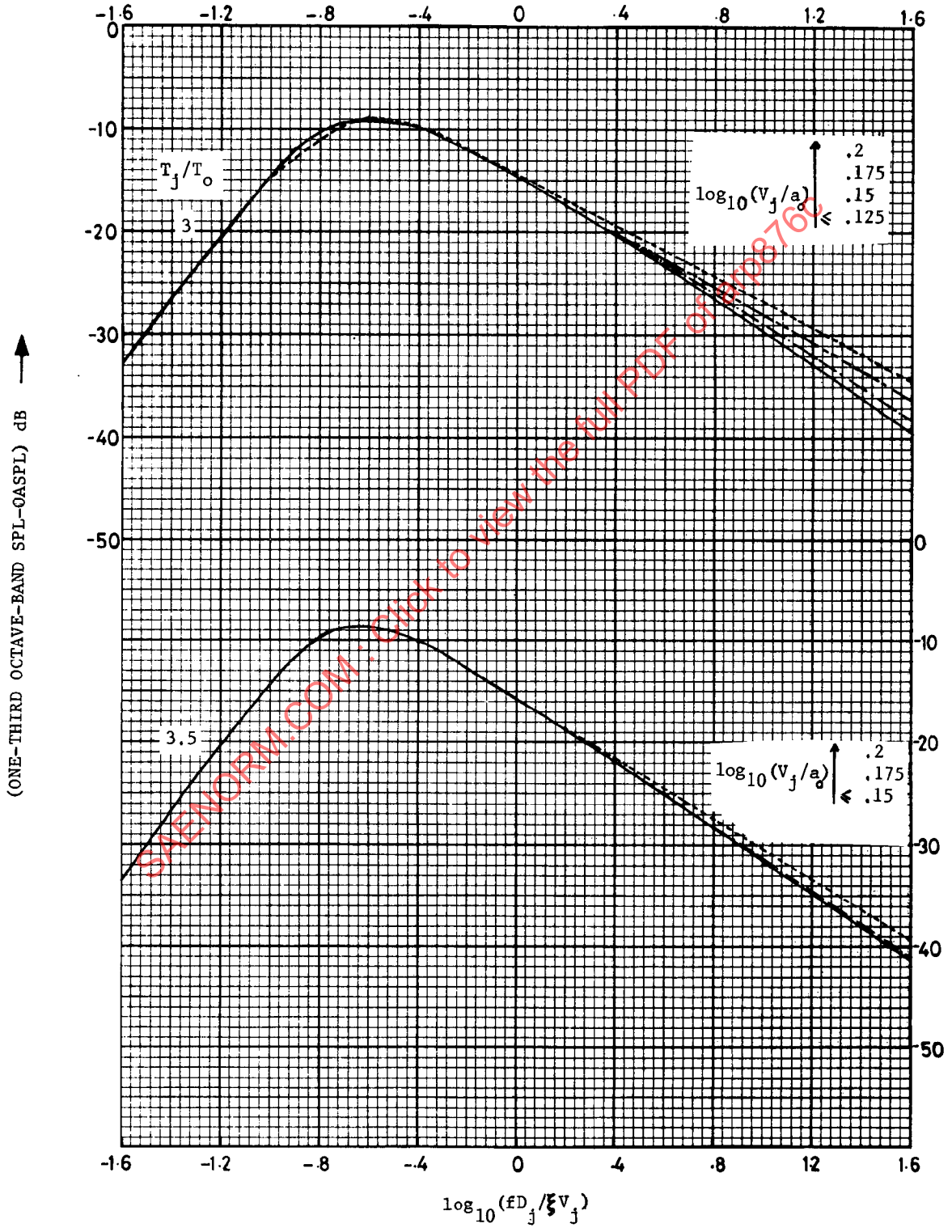

SAENORM.COM : Click to view the full PDF of arp876c

FIGURE A8 (CONT'D)

ONE-THIRD OCTAVE-BAND NORMALISED SPECTRA $\theta_i = 140^\circ$

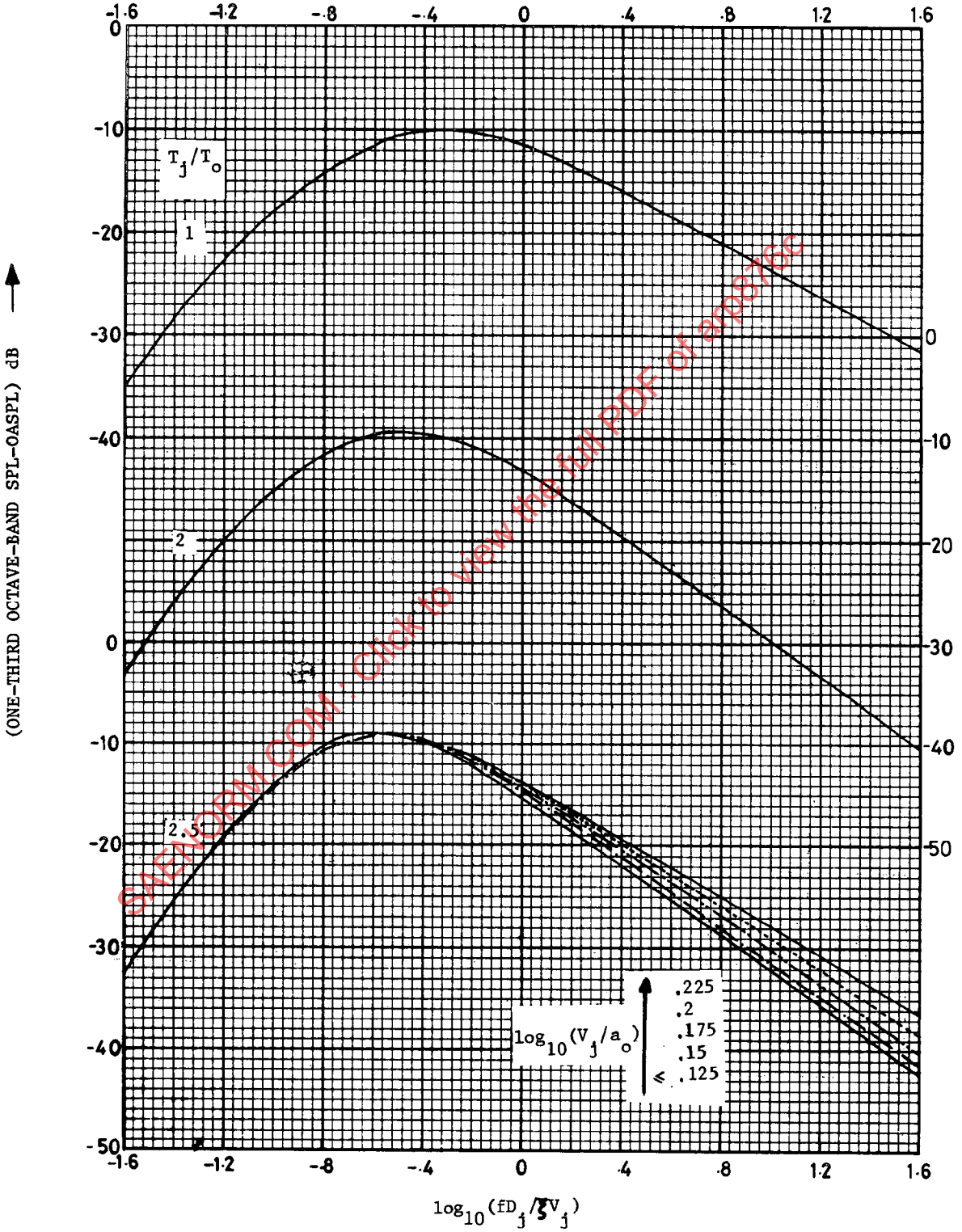

SAENORM.COM : Click to view the full PDF of arp876c

FIGURE A9

ONE-THIRD OCTAVE-BAND NORMALISED SPECTRA $\theta_i = 140°$

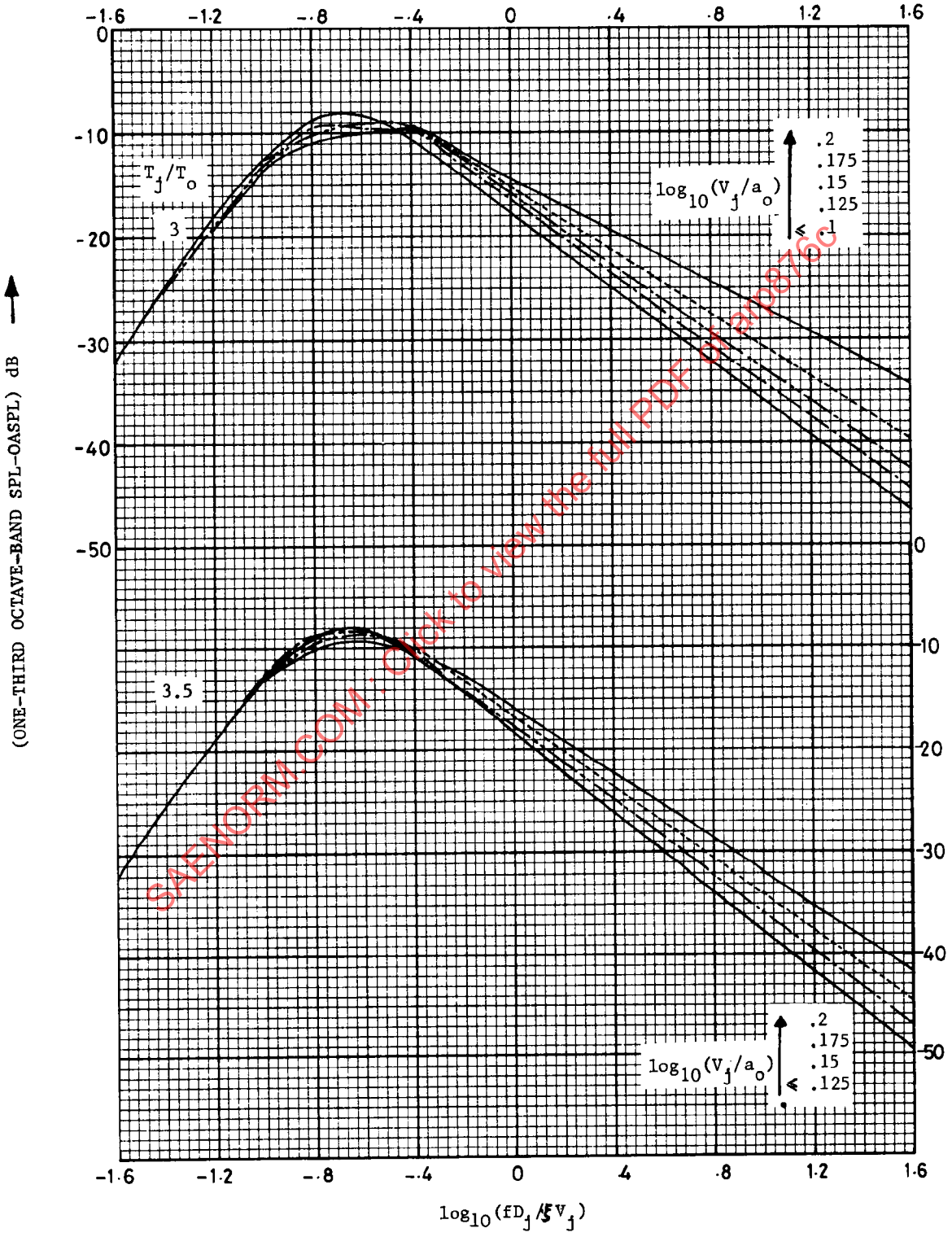

SAENORM.COM : Click to view the full PDF of arp876c

FIGURE A9 (CONT'D)

ONE-THIRD OCTAVE-BAND NORMALISED SPECTRA $\theta_i = 150°$

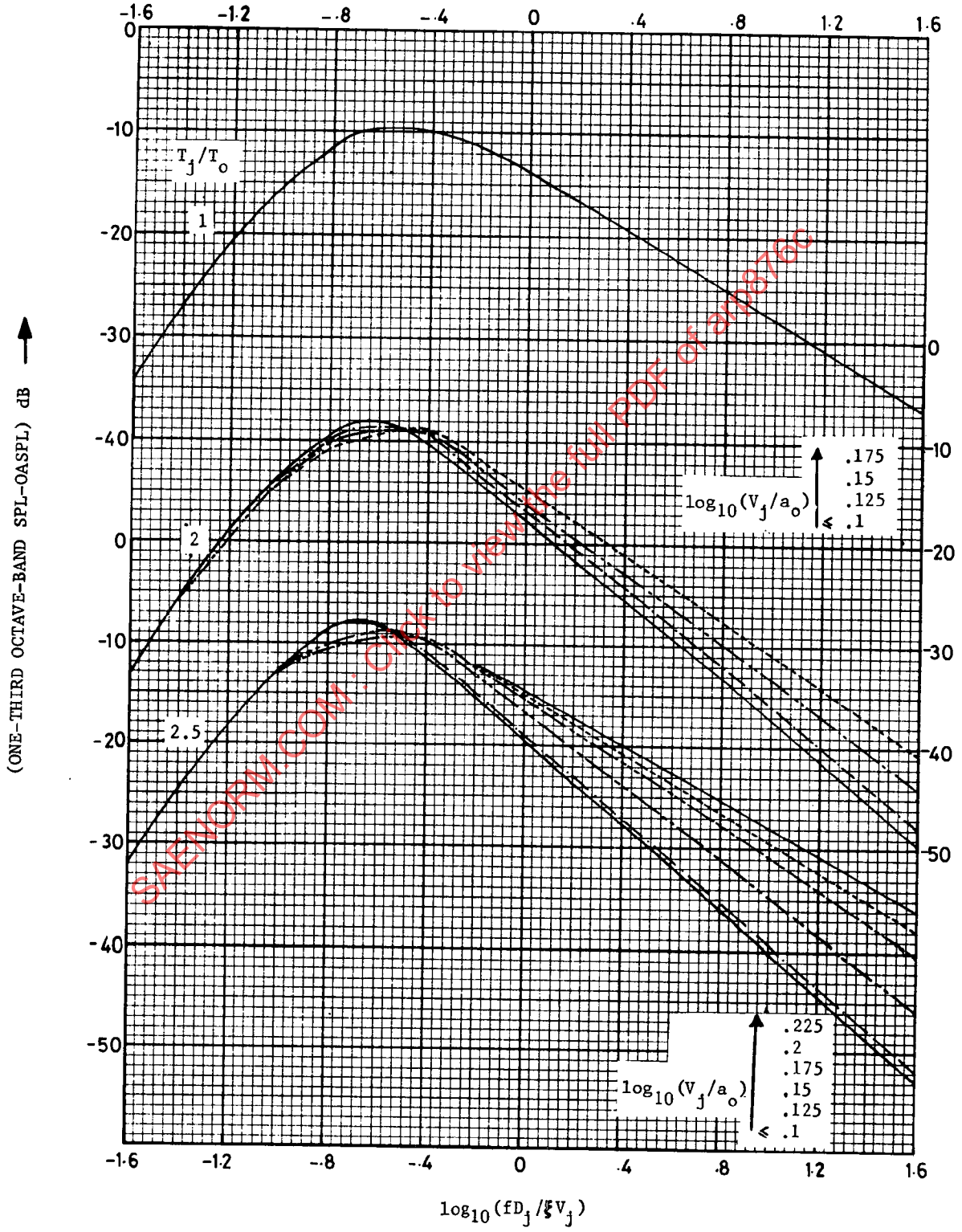

SAENORM.COM : Click to view the full PDF of arp876c

FIGURE A10

ONE-THIRD OCTAVE-BAND NORMALISED SPECTRA $\Theta_i = 150°$

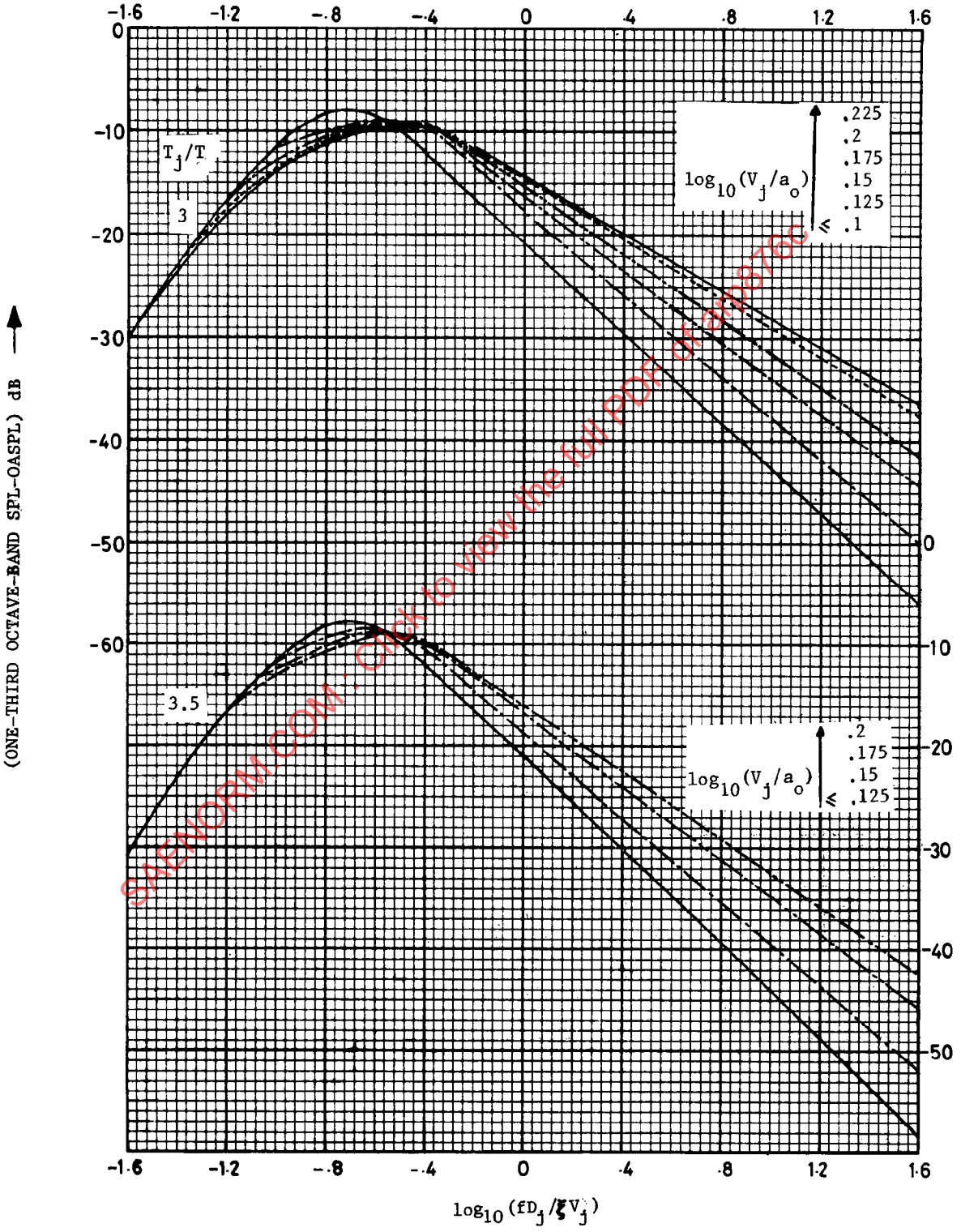

SAENORM.COM : Click to view the full PDF of arp876c

FIGURE 10 (CONT'D)

ONE-THIRD OCTAVE-BAND NORMALISED SPECTRA $\theta_i = 160°$

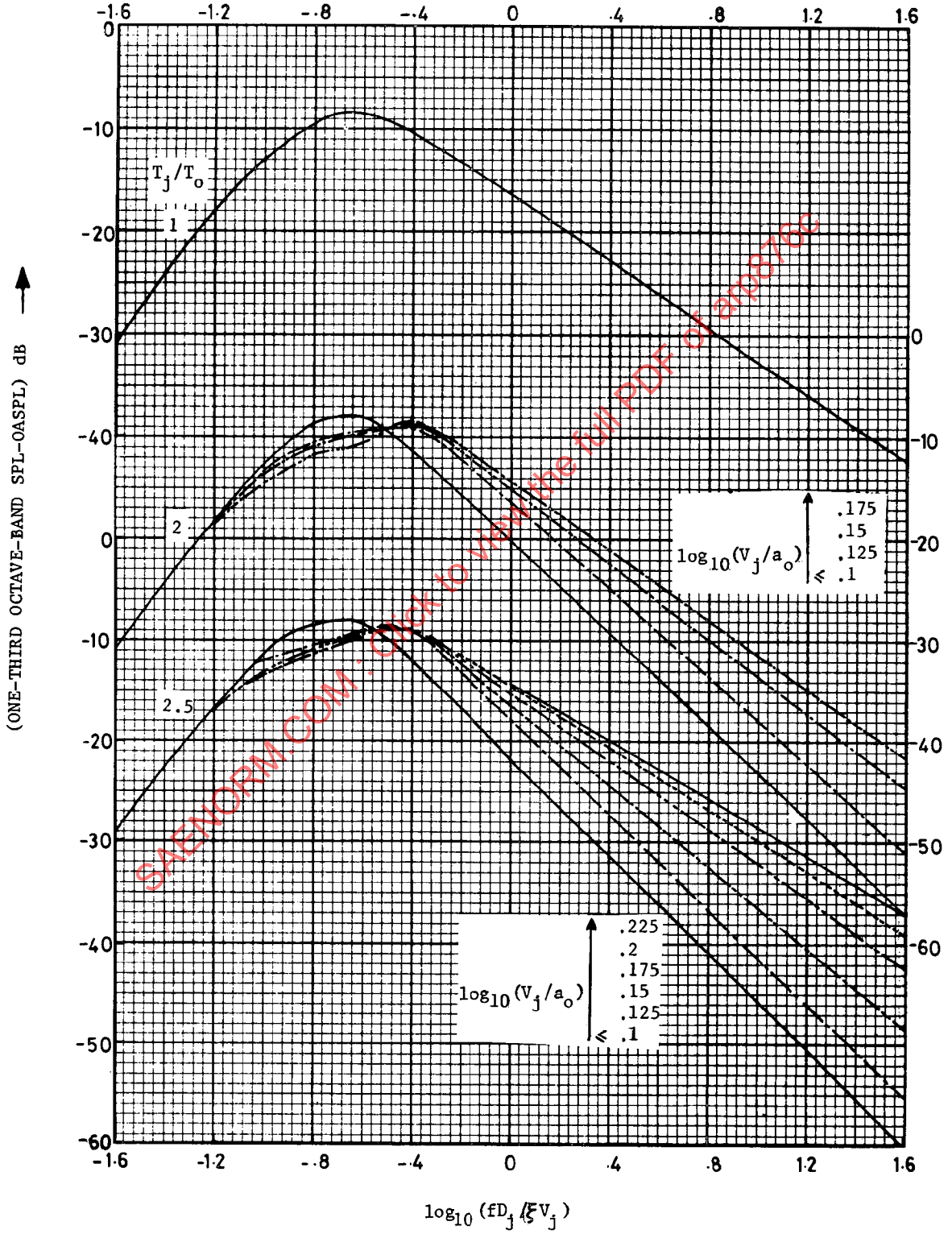

SAENORM.COM : Click to view the full PDF of arp876c

FIGURE A11

ONE-THIRD OCTAVE-BAND NORMALISED SPECTRA $\theta_i = 160°$

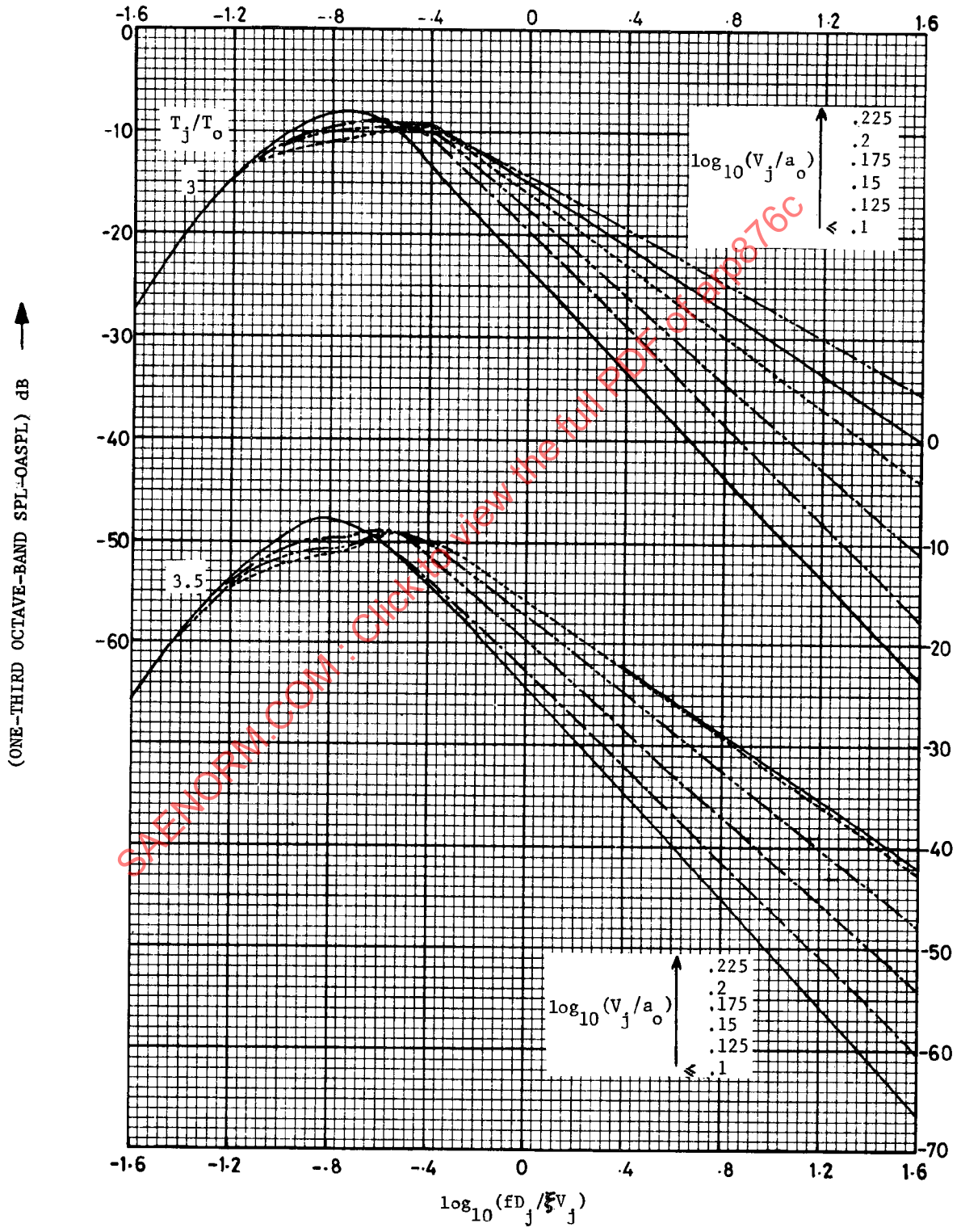

SAENORM.COM : Click to view the full PDF of arp876c

FIGURE 11 (CONT'D)

VARIABLE DENSITY INDEX ω
(REF. FIG. A1)

$\log_{10}(V_j/a_o)$	ω
-.4	-.90
-.35	-.76
-.3	-.58
-.25	-.41
-.20	-.22
-.15	0
-.10	+.22
-.05	+.50
0	+.77
+.05	+1.07
+.10	+1.39
+.15	+1.74
+.20	+1.95
+.25	+2.0
+.30	+2.0
+.35	+2.0
+.40	+2.0

Note: The values of ω in this table have been derived from rig data where jet temperature T_j varied from 288 K to 1100 K.

TABLE A1

SAENORM.COM : Click to view the full PDF of arp876c

PURE JET MIXING NOISE
NON-DIMENSIONAL POLAR OASPL VALUES (REF. FIG. A2)

$\log_{10}(V_j/a_o)$	θ_j, Angle to Inlet														
	20	30	40	50	60	70	80	90	100	110	120	130	140	150	160
-.4	106.6	107.0	107.2	107.5	108.0	108.4	108.8	109.5	110.2	111.2	112.3	113.2	114.0	114.6	114.9
-.35	110.1	110.5	111.0	111.3	111.5	112.1	112.5	113.2	113.9	115.0	116.1	117.2	118.2	118.7	119.2
-.30	113.7	114.1	114.5	115.0	115.4	115.8	116.3	116.8	117.7	118.7	120.0	121.2	122.2	122.9	123.4
-.25	117.3	117.7	118.2	118.5	118.8	119.4	120.0	120.6	121.5	122.6	123.9	125.3	126.5	127.3	127.7
-.20	121.0	121.3	121.7	122.0	122.5	123.0	123.6	124.3	125.3	126.5	128.0	129.5	130.6	131.5	131.9
-.15	124.7	125.0	125.5	125.8	126.2	126.6	127.3	128.1	129.2	130.5	132.1	133.8	135.0	136.0	136.3
-.10	128.4	128.7	129.1	129.5	130.0	130.4	131.0	131.8	133.0	134.5	136.4	138.0	139.5	140.4	140.7
-.05	132.1	132.4	132.8	133.1	133.7	133.9	134.7	135.7	136.9	138.7	140.7	142.7	144.3	145.4	145.3
0	136.0	136.1	136.4	136.7	137.1	137.7	138.4	139.4	140.9	142.8	145.0	147.5	149.3	150.4	150.2
+.05	139.9	140.0	140.3	140.6	141.0	141.4	142.3	143.3	145.0	147.1	149.6	152.3	154.8	156.1	155.4
+.10	143.9	144.0	144.1	144.3	144.6	145.2	146.1	147.4	149.0	151.4	154.2	157.4	160.3	161.9	161.0
+.15	147.5	147.8	148.0	148.3	148.8	149.3	150.3	151.5	153.3	155.8	159.0	162.8	165.8	167.0	165.8
+.20	151.3	151.5	151.9	152.4	152.9	153.7	154.6	155.9	157.7	160.4	164.2	168.5	171.1	171.3	170.0
+.25	154.8	155.2	155.5	156.0	156.7	157.5	158.5	159.9	161.7	164.8	168.8	173.6	175.7	174.9	172.6
+.30	158.1	158.5	159.0	159.5	160.2	161.1	162.2	163.7	165.8	168.9	173.4	178.0	179.6	177.8	174.6
+.35	161.3	161.6	162.1	162.7	163.3	164.3	165.5	167.1	169.3	172.7	177.2	181.5	182.5	180.1	176.2
+.4	164.3	164.5	164.9	165.4	166.0	167.0	168.3	170.0	172.5	176.4	180.6	184.2	183.8	181.4	177.5

TABLE A2

SAENORM.COM : Click to view the full PDF of arp876c

(V_j/a_o)	Values of ξ (See Fig. A3)					
	$\theta_i \leq 120°$	130°	135°	140°	150°	160°
1.4	1.0	1.0	1.0	1.0	1.0	1.0
1.5	1.0	1.0	1.0	1.0	1.0	.995
1.6	1.0	1.0	1.0	1.0	1.0	.885
1.7	1.0	1.0	1.0	1.0	.965	.76
1.8	1.0	1.0	1.0	.99	.87	.66
1.9	1.0	1.0	1.0	.95	.775	.59
2.0	1.0	1.0	.981	.90	.71	.54
2.1	1.0	1.0	.955	.86	.66	.5
2.2	1.0	1.0	.920	.83	.63	.47
2.3	1.0	.985	.895	.81	.61	.445
2.4	1.0	.970	.88	.795	.595	.43
2.5	1.0	.955	.87	.79	.59	.420

For $(V_j/a_o) < 1.4$, $\xi = 1.0$ for all angles

TABLE A3

SAENORM.COM : Click to view the full PDF of arp876c

GAS TURBINE JET EXHAUST NOISE PREDICTION

θ, ANGLE TO INTAKE = 90.00 DEGREES

$\log_{10}(fD_j/\xi V_j)$	ONE-THIRD OCTAVE-BAND SOUND PRESSURE LEVEL (SPL-OASPL) DB				
-1.60	-32.95	-30.09	-30.12	-30.33	-30.23
-1.50	-30.75	-27.91	-27.88	-28.15	-28.04
-1.40	-28.53	-25.83	-25.71	-25.95	-25.81
-1.30	-26.35	-23.79	-23.62	-23.83	-23.63
-1.20	-24.31	-21.77	-21.66	-21.85	-21.57
-1.10	-22.04	-19.85	-19.80	-19.73	-19.41
-1.00	-19.65	-18.09	-18.02	-17.53	-17.23
-0.90	-17.95	-16.64	-16.39	-15.73	-15.47
-0.80	-16.50	-15.24	-14.86	-14.19	-14.00
-0.70	-15.16	-13.80	-13.43	-12.94	-12.84
-0.60	-14.13	-12.57	-12.40	-11.91	-11.81
-0.50	-13.05	-11.79	-11.52	-11.23	-11.23
-0.40	-12.26	-11.30	-11.03	-10.93	-10.83
-0.30	-11.84	-10.99	-10.62	-10.93	-10.83
-0.20	-11.42	-11.00	-10.88	-11.07	-10.84
-0.10	-11.35	-11.12	-11.10	-11.24	-11.13
0.0	-11.35	-11.40	-11.42	-11.53	-11.63
0.10	-11.46	-11.84	-11.94	-12.04	-12.20
0.20	-11.78	-12.44	-12.60	-12.71	-12.86
0.30	-12.24	-13.16	-13.37	-13.51	-13.62
0.40	-12.79	-13.96	-14.23	-14.40	-14.49
0.50	-13.39	-14.79	-15.14	-15.36	-15.46
0.60	-14.08	-15.68	-16.13	-16.40	-16.62
0.70	-14.90	-16.63	-17.20	-17.55	-17.93
0.80	-15.81	-17.64	-18.33	-18.75	-19.33
0.90	-16.80	-18.70	-19.51	-19.99	-20.75
1.00	-17.85	-19.80	-20.72	-21.23	-22.13
1.10	-18.94	-20.95	-21.96	-22.48	-23.45
1.20	-20.10	-22.13	-23.24	-23.74	-24.78
1.30	-21.32	-23.36	-24.55	-25.03	-26.12
1.40	-22.60	-24.63	-25.91	-26.34	-27.45
1.50	-23.94	-25.95	-27.29	-27.68	-28.79
1.60	-25.35	-27.31	-28.72	-29.03	-30.13
(T_j/T_o)	1.00	2.00	2.50	3.00	3.50
$\log_{10}(V_j/a_o)$	$\leq$ 0.400	$\leq$ 0.400	$\leq$ 0.400	$\leq$ 0.400	$\leq$ 0.400

TABLE A4

SAENORM.COM : Click to view the full PDF of arp876c

GAS TURBINE JET EXHAUST NOISE PREDICTION

θ_i ANGLE TO INTAKE = 100.00 DEGREES

$\log_{10}(fD_j/\xi V_j)$	ONE-THIRD OCTAVE-BAND SOUND PRESSURE LEVEL (SPL-OASPL) DB				
-1.60	-33.07	-31.77	-31.12	-31.11	-30.96
-1.50	-30.81	-29.34	-28.67	-28.79	-28.66
-1.40	-28.56	-26.95	-26.34	-26.50	-26.33
-1.30	-26.37	-24.67	-24.12	-24.31	-24.06
-1.20	-24.32	-22.66	-22.09	-22.31	-21.95
-1.10	-22.13	-20.17	-20.13	-20.25	-19.65
-1.00	-19.87	-17.47	-18.22	-18.10	-17.26
-0.90	-18.06	-16.26	-16.47	-16.04	-15.44
-0.80	-16.53	-15.13	-14.83	-14.21	-13.91
-0.70	-15.28	-13.58	-13.33	-12.82	-12.67
-0.60	-14.15	-12.45	-12.20	-11.69	-11.85
-0.50	-13.37	-11.47	-11.42	-10.91	-11.26
-0.40	-12.39	-10.78	-10.82	-10.61	-10.87
-0.30	-11.67	-10.57	-10.72	-10.61	-10.66
-0.20	-11.27	-10.58	-10.73	-10.76	-10.81
-0.10	-11.27	-10.92	-10.97	-11.16	-11.11
0.0	-11.27	-11.47	-11.42	-11.71	-11.56
0.10	-11.40	-12.09	-11.99	-12.33	-12.15
0.20	-11.74	-12.82	-12.70	-13.04	-12.86
0.30	-12.23	-13.63	-13.52	-13.82	-13.67
0.40	-12.80	-14.49	-14.41	-14.68	-14.59
0.50	-13.42	-15.38	-15.33	-15.63	-15.61
0.60	-14.12	-16.32	-16.32	-16.68	-16.78
0.70	-14.93	-17.30	-17.37	-17.83	-18.07
0.80	-15.84	-18.33	-18.48	-19.03	-19.43
0.90	-16.83	-19.39	-19.63	-20.27	-20.81
1.00	-17.87	-20.48	-20.82	-21.51	-22.16
1.10	-18.97	-21.59	-22.04	-22.75	-23.48
1.20	-20.13	-22.73	-23.30	-24.02	-24.81
1.30	-21.35	-23.90	-24.60	-25.31	-26.14
1.40	-22.63	-25.10	-25.93	-26.62	-27.48
1.50	-23.97	-26.33	-27.31	-27.95	-28.82
1.60	-25.37	-27.58	-28.72	-29.31	-30.16
(T_j/T_o)	1.00	2.00	2.50	3.00	3.50
$\log_{10}(V_j/a_o)$	$\leq$ 0.400	$\leq$ 0.400	$\leq$ 0.400	$\leq$ 0.400	$\leq$ 0.400

TABLE A5

SAENORM.COM : Click to view the full PDF of arp876c

GAS TURBINE JET EXHAUST NOISE PREDICTION

θ_i ANGLE TO INTAKE = 110.00 DEGREES

$\log_{10}(fD_j/\xi V_j)$	ONE-THIRD OCTAVE-BAND SOUND PRESSURE LEVEL (SPL-OASPL) DB				
-1.60	-34.57	-32.82	-32.12	-32.30	-32.03
-1.50	-32.12	-30.26	-29.55	-30.12	-29.36
-1.40	-29.69	-27.74	-27.08	-28.14	-26.64
-1.30	-27.27	-25.32	-24.72	-26.00	-24.03
-1.20	-24.87	-23.10	-22.58	-23.43	-21.69
-1.10	-22.40	-20.93	-20.41	-20.73	-19.26
-1.00	-19.97	-18.82	-18.22	-18.10	-16.83
-0.90	-18.18	-16.93	-16.26	-16.04	-15.17
-0.80	-16.57	-15.24	-14.54	-14.31	-13.82
-0.70	-14.98	-13.84	-13.14	-12.81	-12.64
-0.60	-13.75	-12.60	-12.10	-11.70	-11.52
-0.50	-12.67	-11.53	-11.22	-11.05	-11.03
-0.40	-12.08	-10.93	-10.63	-10.70	-10.64
-0.30	-11.57	-10.63	-10.52	-10.50	-10.53
-0.20	-11.45	-10.54	-10.67	-10.52	-10.69
-0.10	-11.39	-10.83	-10.92	-10.98	-11.02
0.0	-11.37	-11.33	-11.32	-11.70	-11.53
0.10	-11.50	-11.90	-11.96	-12.40	-12.24
0.20	-11.83	-12.56	-12.79	-13.16	-13.12
0.30	-12.32	-13.32	-13.73	-13.99	-14.11
0.40	-12.90	-14.15	-14.74	-14.91	-15.18
0.50	-13.51	-15.05	-15.76	-15.95	-16.29
0.60	-14.21	-16.04	-16.81	-17.14	-17.48
0.70	-15.03	-17.13	-17.93	-18.44	-18.76
0.80	-15.94	-18.26	-19.08	-19.81	-20.08
0.90	-16.93	-19.41	-20.25	-21.18	-21.42
1.00	-17.97	-20.54	-21.42	-22.50	-22.73
1.10	-19.06	-21.65	-22.59	-23.77	-24.02
1.20	-20.22	-22.78	-23.77	-25.03	-25.32
1.30	-21.44	-23.91	-24.97	-26.29	-26.62
1.40	-22.72	-25.04	-26.17	-27.53	-27.92
1.50	-24.06	-26.19	-27.39	-28.77	-29.22
1.60	-25.47	-27.34	-28.62	-30.00	-30.53
(T_j/T_o)	1.00	2.00	2.50	3.00	3.50
$\log_{10}(V_j/a_o)$	$\leq$ 0.400	$\leq$ 0.400	$\leq$ 0.400	$\leq$ 0.400	$\leq$ 0.400

TABLE A6

SAENORM.COM : Click to view the full PDF of arp876c

GAS TURBINE JET EXHAUST NOISE PREDICTION

θ, ANGLE TO INTAKE = 120.00 DEGREES

$\log_{10}(fD_j/\xi V_j)$	ONE-THIRD OCTAVE-BAND SOUND PRESSURE LEVEL (SPL-OASPL) DB				
-1.60	-36.37	-33.75	-33.11	-32.50	-32.27
-1.50	-33.31	-31.00	-30.17	-29.66	-29.32
-1.40	-30.18	-28.25	-27.25	-26.97	-26.44
-1.30	-27.27	-25.65	-24.51	-24.50	-23.66
-1.20	-24.82	-23.35	-22.16	-22.52	-21.11
-1.10	-22.49	-21.13	-19.75	-20.30	-18.56
-1.00	-20.27	-18.95	-17.31	-17.80	-16.06
-0.90	-18.50	-16.88	-15.31	-15.63	-13.99
-0.80	-16.87	-15.06	-13.63	-13.82	-12.31
-0.70	-15.29	-13.66	-12.32	-12.51	-11.17
-0.60	-14.05	-12.43	-11.29	-11.28	-10.45
-0.50	-13.07	-11.35	-10.61	-10.60	-10.06
-0.40	-12.28	-10.76	-10.31	-10.30	-9.97
-0.30	-11.77	-10.46	-10.31	-10.30	-10.17
-0.20	-11.53	-10.37	-10.47	-10.46	-10.71
-0.10	-11.35	-10.65	-10.98	-10.88	-11.40
0.0	-11.27	-11.16	-11.71	-11.50	-12.27
0.10	-11.39	-11.79	-12.56	-12.29	-13.38
0.20	-11.71	-12.55	-13.54	-13.23	-14.67
0.30	-12.17	-13.42	-14.61	-14.30	-16.06
0.40	-12.72	-14.38	-15.74	-15.46	-17.49
0.50	-13.31	-15.41	-16.87	-16.69	-18.89
0.60	-14.01	-16.55	-18.03	-18.04	-20.29
0.70	-14.82	-17.79	-19.24	-19.50	-21.72
0.80	-15.74	-19.08	-20.48	-21.02	-23.17
0.90	-16.73	-20.39	-21.74	-22.56	-24.62
1.00	-17.77	-21.67	-23.00	-24.10	-26.07
1.10	-18.87	-22.94	-24.28	-25.63	-27.51
1.20	-20.02	-24.21	-25.58	-27.17	-28.96
1.30	-21.24	-25.49	-26.88	-28.73	-30.41
1.40	-22.52	-26.78	-28.21	-30.31	-31.86
1.50	-23.87	-28.08	-29.55	-31.90	-33.31
1.60	-25.27	-29.38	-30.90	-33.50	-34.77
(T_j/T_o)	1.00	2.00	2.50	3.00	3.50
$\log_{10}(V_j/a_o)$	$\leq$ 0.400	$\leq$ 0.400	$\leq$ 0.400	$\leq$ 0.400	$\leq$ 0.400

TABLE A7

SAENORM.COM : Click to view the full PDF of arp876c

GAS TURBINE JET EXHAUST NOISE PREDICTION

θ_i ANGLE TO INTAKE = 130.00 DEGREES

$\log_{10}(fD_j/\varepsilon V_j)$	ONE-THIRD OCTAVE-BAND SOUND PRESSURE LEVEL (SPL-OASPL) DB									
-1.60	-35.40	-34.33	-33.16	-32.65	-32.67	-32.69	-32.70	-33.44	-33.44	-33.45
-1.50	-32.25	-31.23	-29.91	-29.53	-29.55	-29.57	-29.58	-30.18	-30.18	-30.19
-1.40	-29.26	-28.17	-26.69	-26.54	-26.55	-26.57	-26.59	-26.93	-26.93	-26.94
-1.30	-26.50	-25.23	-23.66	-23.65	-23.67	-23.69	-23.70	-23.74	-23.74	-23.75
-1.20	-24.17	-22.51	-21.01	-21.04	-21.05	-21.08	-21.09	-20.69	-20.69	-20.70
-1.10	-22.02	-19.97	-18.51	-18.01	-18.02	-18.04	-18.06	-17.45	-17.45	-17.46
-1.00	-20.00	-17.63	-16.16	-14.65	-14.66	-14.69	-14.70	-14.14	-14.14	-14.15
-0.90	-18.24	-15.60	-14.14	-11.87	-11.88	-11.90	-12.58	-11.37	-11.37	-11.50
-0.80	-16.60	-13.82	-12.35	-10.05	-10.06	-10.08	-11.15	-9.51	-9.51	-9.70
-0.70	-15.01	-12.34	-10.87	-9.36	-9.37	-9.39	-9.71	-8.74	-8.74	-8.75
-0.60	-13.77	-11.21	-10.15	-9.15	-9.16	-9.19	-8.70	-8.64	-8.64	-8.65
-0.50	-12.50	-10.43	-9.76	-9.25	-9.27	-9.29	-9.00	-9.04	-9.06	-8.95
-0.40	-11.61	-10.14	-9.85	-9.94	-9.95	-9.97	-9.78	-10.21	-10.21	-10.23
-0.30	-10.99	-10.14	-10.17	-10.87	-10.88	-10.90	-10.91	-11.45	-11.45	-11.46
-0.20	-10.80	-10.21	-10.84	-11.92	-11.93	-11.95	-11.97	-12.64	-12.64	-12.65
-0.10	-10.84	-10.70	-11.73	-13.25	-13.26	-13.23	-13.29	-14.15	-14.15	-14.16
0.0	-11.00	-11.44	-12.76	-14.66	-14.67	-14.69	-14.70	-15.74	-15.74	-15.75
0.10	-11.35	-12.40	-13.89	-16.08	-16.08	-16.08	-16.02	-17.30	-17.31	-17.25
0.20	-11.91	-13.54	-15.06	-17.54	-17.50	-17.45	-17.20	-18.87	-18.88	-18.68
0.30	-12.61	-14.80	-16.27	-19.01	-18.92	-18.80	-18.31	-20.44	-20.45	-20.06
0.40	-13.38	-16.13	-17.50	-20.50	-20.36	-20.15	-19.41	-22.02	-22.03	-21.45
0.50	-14.18	-17.46	-18.75	-22.00	-21.80	-21.50	-20.58	-23.61	-23.60	-22.89
0.60	-15.02	-18.83	-20.04	-23.51	-23.26	-22.85	-21.79	-25.19	-25.17	-24.37
0.70	-15.93	-20.27	-21.36	-25.03	-24.73	-24.19	-23.01	-26.77	-26.73	-25.86
0.80	-16.89	-21.73	-22.69	-26.56	-26.21	-25.53	-24.24	-28.35	-28.30	-27.36
0.90	-17.92	-23.21	-24.03	-28.11	-27.69	-26.86	-25.47	-29.94	-29.87	-28.86
1.00	-19.00	-24.66	-25.36	-29.66	-29.17	-28.19	-26.71	-31.54	-31.44	-30.35
1.10	-20.12	-26.09	-26.67	-31.22	-30.66	-29.53	-27.95	-33.15	-33.02	-31.83
1.20	-21.30	-27.53	-27.97	-32.79	-32.16	-30.87	-29.19	-34.76	-34.60	-33.31
1.30	-22.52	-28.96	-29.27	-34.37	-33.66	-32.20	-30.44	-36.38	-36.19	-34.78
1.40	-23.80	-30.39	-30.57	-35.96	-35.16	-33.53	-31.69	-37.99	-37.77	-36.24
1.50	-25.12	-31.83	-31.86	-37.55	-36.67	-34.87	-32.95	-39.61	-39.36	-37.70
1.60	-26.50	-33.26	-33.15	-39.16	-38.18	-36.20	-34.21	-41.24	-40.95	-39.16
(T_j/T_o)	1.00	2.00	2.50	3.00	3.00	3.00	3.00	3.50	3.50	3.50
$\log_{10}(V_j/a_o)$	$\leq$ 0.400	$\leq$ 0.400	$\leq$ 0.400	$\leq$ 0.125	0.150	0.175	0.200	$\leq$ 0.150	0.175	0.200

TABLE A8

SAENORM.COM : Click to view the full PDF of arp876c

GAS TURBINE JET EXHAUST NOISE PREDICTION

θ, ANGLE TO INTAKE = 140.00 DEGREES

$\log_{10}(fD_j/\xi V_j)$	ONE-THIRD OCTAVE-BAND SOUND PRESSURE LEVEL (SPL-OASPL) DB											
-1.60	-35.00	-32.65	-32.39	-32.45	-32.63	-32.73	-32.80	-31.96	-31.60	-31.66	-31.67	-31.77
-1.50	-31.51	-29.09	-28.90	-28.95	-29.14	-29.23	-29.30	-28.59	-28.23	-28.29	-28.30	-28.40
-1.40	-28.16	-25.66	-25.43	-25.49	-25.67	-25.77	-25.84	-25.30	-24.94	-25.00	-25.01	-25.10
-1.30	-25.10	-22.55	-22.19	-22.25	-22.43	-22.53	-22.60	-22.16	-21.80	-21.86	-21.87	-21.97
-1.20	-22.65	-20.10	-19.42	-19.48	-19.66	-19.76	-19.83	-19.41	-19.06	-19.12	-19.13	-19.22
-1.10	-20.28	-17.68	-16.69	-16.75	-16.93	-17.03	-17.09	-16.17	-15.84	-15.96	-16.01	-16.16
-1.00	-17.90	-15.24	-13.99	-14.05	-14.23	-14.33	-14.40	-12.66	-12.50	-12.86	-13.07	-13.47
-0.90	-15.85	-13.31	-11.73	-12.14	-12.33	-12.43	-12.49	-10.35	-10.60	-11.18	-11.45	-12.01
-0.80	-14.15	-11.64	-10.08	-10.73	-10.92	-11.01	-11.08	-8.88	-9.60	-10.13	-10.47	-11.04
-0.70	-12.92	-10.25	-9.20	-9.85	-10.04	-10.14	-10.20	-8.26	-9.20	-9.56	-9.97	-10.46
-0.60	-11.58	-9.64	-8.99	-9.24	-9.43	-9.53	-9.59	-8.26	-9.70	-9.25	-9.56	-10.05
-0.50	-10.60	-9.45	-9.09	-9.15	-9.33	-9.43	-9.50	-9.16	-8.30	-8.76	-9.17	-9.57
-0.40	-10.21	-9.74	-9.88	-9.54	-9.62	-9.72	-9.79	-10.63	-9.70	-9.33	-9.36	-9.46
-0.30	-9.90	-10.16	-10.90	-10.26	-10.24	-10.34	-10.41	-12.48	-11.33	-11.08	-10.49	-10.38
-0.20	-10.19	-10.97	-12.20	-11.76	-11.42	-11.49	-11.35	-14.14	-13.17	-12.74	-12.25	-11.76
-0.10	-10.64	-12.02	-13.65	-13.21	-12.78	-12.67	-12.63	-15.88	-14.70	-14.35	-13.80	-13.02
0.0	-11.30	-13.26	-15.19	-14.75	-14.23	-13.93	-14.00	-17.66	-16.31	-15.97	-15.28	-14.27
0.10	-12.23	-14.68	-16.82	-16.33	-15.76	-15.33	-15.33	-19.47	-18.15	-17.65	-16.78	-15.56
0.20	-13.37	-16.22	-18.52	-17.89	-17.35	-16.81	-16.67	-21.30	-20.06	-19.35	-18.27	-16.87
0.30	-14.63	-17.84	-20.24	-19.46	-18.96	-18.33	-18.00	-23.13	-21.99	-21.06	-19.75	-18.18
0.40	-15.93	-19.49	-21.97	-21.07	-20.59	-19.36	-19.35	-24.97	-23.90	-22.77	-21.23	-19.48
0.50	-17.19	-21.15	-23.68	-22.75	-22.21	-21.38	-20.71	-26.77	-25.72	-24.46	-22.73	-20.76
0.60	-18.46	-22.83	-25.38	-24.45	-23.82	-22.89	-22.09	-28.56	-27.44	-26.14	-24.23	-22.02
0.70	-19.76	-24.55	-27.08	-26.14	-25.45	-24.42	-23.47	-20.33	-29.07	-27.81	-25.74	-23.26
0.80	-21.08	-26.28	-28.78	-27.85	-27.07	-25.95	-24.87	-32.10	-30.67	-29.47	-27.26	-24.49
0.90	-22.40	-28.03	-30.48	-29.55	-28.71	-27.49	-26.28	-33.87	-32.27	-31.13	-28.77	-25.73
1.00	-23.70	-29.77	-32.19	-31.26	-30.34	-29.03	-27.70	-35.66	-33.92	-32.78	-30.29	-26.97
1.10	-24.99	-31.51	-33.90	-32.96	-31.97	-30.58	-29.14	-37.47	-35.61	-34.42	-31.80	-28.22
1.20	-26.28	-33.25	-35.61	-34.66	-33.60	-32.14	-30.59	-39.29	-37.33	-36.05	-33.32	-29.47
1.30	-27.57	-35.00	-37.33	-36.36	-35.23	-33.70	-32.05	-41.12	-39.05	-37.67	-34.83	-30.72
1.40	-28.85	-36.76	-39.05	-38.06	-36.87	-35.27	-33.52	-42.96	-40.79	-39.28	-36.35	-31.97
1.50	-30.13	-38.51	-40.77	-39.76	-38.50	-36.85	-35.00	-44.81	-42.55	-40.89	-37.87	-33.22
1.60	-31.40	-40.28	-42.49	-41.46	-40.14	-38.43	-36.50	-46.66	-44.32	-42.48	-39.39	-34.47
(T_j/T_o)	1.00	2.00	2.50	2.50	2.50	2.50	2.50	3.00	3.00	3.00	3.00	3.00
$\log_{10}(V_j/a_o)$	$\leq$ 0.400	$\leq$ 0.400	$\leq$ 0.125	0.150	0.175	0.200	0.225	$\leq$ 0.100	0.125	0.150	0.175	0.200

SAENORM.COM : Click to view the full PDF of arp876c

TABLE A9

GAS TURBINE JET EXHAUST NOISE PREDICTION

θ ¿ ANGLE TO INTAKE = 140.00 DEGREES

$\log_{10}(fD_j/\xi V_j)$	ONE-THIRD OCTAVE-BAND SOUND PRESSURE LEVEL (SPL-OASPL) DB				
-1.60	-32.16	-32.14	-31.97	-31.89	-31.75
-1.50	-28.71	-28.69	-28.52	-28.44	-28.30
-1.40	-25.31	-25.29	-25.12	-25.04	-24.90
-1.30	-22.06	-22.04	-21.87	-21.79	-21.65
-1.20	-19.13	-19.11	-18.94	-18.86	-18.72
-1.10	-16.03	-16.02	-15.85	-15.77	-15.63
-1.00	-12.86	-12.84	-12.77	-12.69	-12.65
-0.90	-10.32	-10.34	-10.68	-10.75	-11.08
-0.80	-8.67	-8.77	-9.28	-9.69	-10.27
-0.70	-8.06	-8.24	-8.57	-9.29	-9.85
-0.60	-8.16	-8.24	-8.37	-8.58	-9.13
-0.50	-8.76	-8.64	-8.57	-8.59	-8.45
-0.40	-10.82	-10.70	-10.03	-9.96	-9.82
-0.30	-12.88	-12.66	-12.39	-11.61	-11.17
-0.20	-14.67	-14.55	-14.18	-13.39	-12.81
-0.10	-16.61	-16.43	-15.99	-15.16	-14.39
0.0	-18.56	-18.35	-17.78	-16.89	-15.95
0.10	-20.47	-20.27	-19.56	-18.64	-17.54
0.20	-22.37	-22.19	-21.33	-20.39	-19.12
0.30	-24.27	-24.12	-23.10	-22.13	-20.72
0.40	-26.18	-26.05	-24.88	-23.86	-22.32
0.50	-28.11	-27.99	-26.70	-25.59	-23.92
0.60	-30.07	-29.94	-28.56	-27.30	-25.54
0.70	-32.04	-31.90	-30.44	-28.99	-27.17
0.80	-34.03	-33.86	-32.34	-30.67	-28.81
0.90	-36.00	-35.81	-34.22	-32.37	-30.44
1.00	-37.96	-37.75	-36.09	-34.10	-32.06
1.10	-39.90	-39.67	-37.93	-35.84	-33.67
1.20	-41.83	-41.58	-39.76	-37.60	-35.27
1.30	-43.75	-43.49	-41.58	-39.36	-36.88
1.40	-45.66	-45.39	-43.40	-41.13	-38.48
1.50	-47.57	-47.27	-45.20	-42.91	-40.07
1.60	-49.46	-49.15	-46.99	-44.70	-41.66
(T_j/T_o)	3.50	3.50	3.50	3.50	3.50
$\log_{10}(V_j/a_o)$	$\leq$ 0.100	0.125	0.150	0.175	0.200

TABLE A9 (CONTINUED)

SAENORM.COM : Click to view the full PDF of arp876c

GAS TURBINE JET EXHAUST NOISE PREDICTION

θ, ANGLE TO INTAKE = 150.00 DEGREES

$\log_{10}(fD_j/\xi V_j)$	ONE-THIRD OCTAVE-BAND SOUND PRESSURE LEVEL (SPL-OASPL) DB											
-1.60	-34.07	-33.04	-32.98	-33.20	-33.20	-31.93	-31.84	-31.40	-31.60	-31.74	-31.88	-29.85
-1.50	-30.40	-29.37	-29.30	-29.53	-29.52	-28.33	-28.24	-27.80	-28.00	-28.14	-28.27	-26.37
-1.40	-26.80	-25.71	-25.65	-25.88	-25.87	-24.72	-24.63	-24.19	-24.39	-24.53	-24.67	-23.07
-1.30	-23.47	-22.24	-22.18	-22.40	-22.40	-21.33	-21.24	-20.80	-21.00	-21.14	-21.28	-19.85
-1.20	-20.69	-19.09	-19.03	-19.26	-19.25	-18.42	-18.33	-17.89	-18.09	-18.23	-18.37	-16.65
-1.10	-17.96	-16.26	-16.20	-16.42	-16.45	-15.59	-15.50	-15.11	-15.31	-15.45	-15.58	-13.69
-1.00	-15.27	-13.74	-13.67	-13.90	-14.10	-12.83	-12.74	-12.70	-12.90	-13.04	-13.18	-11.15
-0.90	-13.13	-11.51	-11.55	-11.78	-12.20	-10.39	-10.33	-11.24	-11.56	-11.70	-11.84	-9.27
-0.80	-11.37	-9.62	-9.97	-10.20	-10.86	-8.57	-8.62	-10.26	-10.67	-10.81	-10.95	-8.17
-0.70	-10.07	-8.25	-9.18	-9.42	-10.22	-7.63	-7.94	-9.60	-10.00	-10.14	-10.28	-7.85
-0.60	-9.47	-7.75	-8.68	-8.91	-9.70	-7.74	-7.94	-8.68	-9.19	-9.33	-9.46	-8.37
-0.50	-9.47	-8.45	-8.48	-8.71	-9.41	-9.13	-9.14	-8.50	-8.90	-9.04	-9.18	-9.85
-0.40	-9.76	-10.22	-9.16	-8.98	-8.69	-11.29	-10.90	-9.37	-9.38	-9.52	-9.66	-12.10
-0.30	-10.27	-11.97	-10.91	-10.94	-10.13	-13.25	-12.86	-11.43	-11.02	-10.86	-10.89	-14.17
-0.20	-11.29	-13.88	-13.12	-12.50	-11.55	-15.28	-14.99	-18.20	-12.43	-12.26	-12.16	-16.54
-0.10	-12.32	-15.81	-14.96	-14.25	-13.17	-17.35	-17.02	-15.01	-14.02	-13.70	-13.47	-18.71
0.0	-13.47	-17.76	-16.81	-16.03	-14.81	-19.43	-19.05	-16.81	-15.60	-15.14	-14.78	-20.85
0.10	-14.82	-19.75	-18.71	-17.79	-16.41	-21.50	-21.09	-18.58	-17.11	-16.57	-16.08	-23.02
0.20	-16.29	-21.75	-20.63	-19.56	-18.00	-23.58	-23.15	-20.34	-18.59	-18.00	-17.38	-25.20
0.30	-17.81	-23.76	-22.57	-21.33	-19.59	-25.65	-25.21	-22.09	-20.06	-19.42	-18.67	-27.38
0.40	-19.33	-25.75	-24.51	-23.09	-21.18	-27.73	-27.27	-23.85	-21.54	-20.84	-19.97	-29.57
0.50	-20.79	-27.72	-26.46	-24.84	-22.78	-29.81	-29.32	-25.64	-23.06	-22.27	-21.23	-31.75
0.60	-22.20	-29.64	-28.41	-26.57	-24.40	-31.89	-31.36	-27.44	-24.61	-23.71	-22.60	-33.93
0.70	-23.59	-31.54	-30.36	-28.29	-26.04	-33.98	-33.40	-29.26	-26.18	-25.14	-23.91	-36.10
0.80	-24.97	-33.43	-32.31	-30.00	-27.67	-36.07	-35.44	-31.09	-27.77	-26.58	-25.24	-38.28
0.90	-26.36	-35.34	-34.26	-31.72	-29.30	-38.15	-37.49	-32.91	-29.35	-28.01	-26.56	-40.46
1.00	-27.77	-37.28	-36.23	-33.45	-30.91	-40.23	-39.55	-34.73	-30.91	-29.44	-27.88	-42.65
1.10	-29.19	-39.25	-38.18	-35.19	-32.51	-42.30	-41.62	-36.54	-32.46	-30.87	-29.20	-44.84
1.20	-30.63	-41.25	-40.13	-36.93	-34.11	-44.37	-43.69	-38.35	-34.00	-32.29	-30.51	-47.04
1.30	-32.07	-43.26	-42.06	-38.68	-35.69	-46.44	-45.75	-40.15	-35.54	-33.71	-31.83	-49.23
1.40	-33.53	-45.28	-43.99	-40.44	-37.27	-48.51	-47.81	-41.95	-37.07	-35.12	-33.15	-51.44
1.50	-34.99	-47.33	-45.91	-42.20	-38.85	-50.57	-49.88	-43.75	-38.59	-36.53	-34.46	-53.64
1.60	-36.47	-49.39	-47.84	-43.96	-40.41	-52.63	-51.95	-45.54	-40.11	-37.94	-35.78	-55.85
(T_j/T_o)	1.00	2.00	2.00	2.00	2.00	2.50	2.50	2.50	2.50	2.50	2.50	3.00
$\log_{10}(V_j/a_o)$	$\leq$ 0.400	$\leq$ 0.100	0.125	0.150	0.175	$\leq$ 0.100	0.125	0.150	0.175	0.200	0.225	$\leq$ 0.100

SAENORM.COM : Click to view the full PDF of arp876c

TABLE A10

GAS TURBINE JET EXHAUST NOISE PREDICTION

θ ¿ ANGLE TO INTAKE = 150.00 DEGREES

$\log_{10}(fD_j/\varepsilon V_j)$	ONE-THIRD OCTAVE-BAND SOUND PRESSURE LEVEL (SPL-OASPL) DB									
-1.60	-29.97	-29.98	-30.03	-30.02	-30.07	-30.64	-30.39	-30.40	-30.39	-30.40
-1.50	-26.49	-26.50	-26.56	-26.58	-26.65	-26.86	-26.51	-26.62	-26.62	-26.62
-1.40	-23.20	-23.21	-23.26	-23.38	-23.53	-23.14	-22.89	-22.90	-22.89	-22.92
-1.30	-19.97	-19.98	-20.03	-20.32	-20.56	-19.64	-19.39	-19.39	-19.39	-19.50
-1.20	-16.89	-17.06	-17.23	-17.53	-17.87	-16.61	-16.46	-16.74	-16.69	-16.82
-1.10	-14.06	-14.54	-14.90	-15.25	-15.51	-13.91	-13.97	-14.40	-14.57	-14.65
-1.00	-11.66	-12.47	-13.03	-13.52	-13.56	-11.53	-11.88	-12.29	-12.89	-12.90
-0.90	-10.69	-11.24	-11.74	-12.24	-12.27	-9.41	-10.31	-10.98	-11.63	-11.63
-0.80	-10.07	-10.38	-10.84	-11.33	-11.37	-8.15	-9.28	-10.09	-10.69	-10.70
-0.70	-9.27	-9.58	-10.14	-10.53	-10.57	-7.83	-8.68	-9.40	-9.90	-9.91
-0.60	-8.86	-9.07	-9.32	-9.51	-9.75	-8.25	-8.48	-8.78	-8.88	-8.88
-0.50	-8.87	-8.98	-9.13	-9.22	-9.37	-9.64	-8.79	-8.79	-8.79	-8.80
-0.40	-9.63	-9.45	-9.52	-9.51	-9.55	-11.90	-10.55	-9.97	-9.67	-9.67
-0.30	-11.70	-11.10	-10.55	-10.43	-10.38	-14.07	-12.72	-11.62	-11.11	-11.12
-0.20	-13.63	-12.88	-12.09	-11.83	-11.66	-16.57	-14.65	-13.30	-12.75	-12.75
-0.10	-15.65	-14.69	-13.77	-13.22	-13.00	-18.82	-16.72	-15.15	-14.37	-14.32
0.0	-17.68	-16.49	-15.44	-14.62	-14.37	-21.05	-18.80	-17.00	-16.00	-15.90
0.10	-19.74	-18.28	-17.05	-16.05	-15.76	-23.36	-20.86	-18.77	-17.62	-17.52
0.20	-21.81	-20.08	-18.64	-17.50	-17.17	-25.69	-22.92	-20.51	-19.25	-19.15
0.30	-23.87	-21.86	-20.22	-18.96	-18.59	-28.04	-24.98	-22.23	-20.88	-20.79
0.40	-25.93	-23.64	-21.81	-20.41	-20.00	-30.37	-27.03	-23.95	-22.52	-22.43
0.50	-27.96	-25.40	-23.41	-21.85	-21.38	-32.68	-29.09	-25.71	-24.18	-24.08
0.60	-29.95	-27.13	-25.03	-23.29	-22.73	-34.94	-31.14	-27.50	-25.86	-25.74
0.70	-31.92	-28.85	-26.65	-24.73	-24.07	-37.17	-33.19	-29.29	-27.55	-27.41
0.80	-33.87	-30.56	-28.28	-26.16	-25.39	-39.40	-35.23	-31.10	-29.24	-29.08
0.90	-35.83	-32.28	-29.91	-27.60	-26.72	-41.65	-37.28	-32.91	-30.93	-39.75
1.00	-37.80	-34.00	-31.54	-29.02	-28.07	-43.96	-39.32	-34.71	-32.60	-32.41
1.10	-39.79	-35.74	-33.18	-30.45	-29.43	-46.30	-41.36	-36.51	-34.25	-34.05
1.20	-41.79	-37.49	-34.81	-31.87	-30.81	-48.63	-43.40	-38.31	-35.90	-35.69
1.30	-43.79	-39.24	-36.44	-33.29	-32.19	-50.97	-45.44	-40.11	-37.54	-37.33
1.40	-45.79	-40.99	-38.08	-34.70	-33.57	-53.32	-47.47	-41.91	-39.17	-38.96
1.50	-47.80	-42.75	-39.71	-36.11	-34.97	-55.68	-49.51	-43.71	-40.79	-49.59
1.60	-49.81	-44.51	-41.35	-37.52	-36.37	-58.07	-51.54	-45.51	-42.40	-42.21
(T_j/T_o)	3.00	3.00	3.00	3.00	3.00	3.50	3.50	3.50	3.50	3.50
$\log_{10}(V_j/a_o)$	0.125	0.150	0.175	0.200	0.225	≤ 0.125	0.150	0.175	0.200	0.225

TABLE A10 (CONTINUED)

SAENORM.COM : Click to view the full PDF of arp876c

GAS TURBINE JET EXHAUST NOISE PREDICTION

θ_i ANGLE TO INTAKE = 160.00 DEGREES

ONE-THIRD OCTAVE-BAND SOUND PRESSURE LEVEL (SPL-OASPL) DB

$\log_{10}(fD_j/\varepsilon V_j)$												
-1.60	-30.74	-30.49	-30.08	-30.50	-30.50	-29.05	-28.90	-29.05	-29.20	-29.38	-29.48	-27.13
-1.50	-27.37	-27.40	-26.99	-27.41	-27.41	-25.76	-25.60	-25.75	-25.90	-26.09	-26.18	-23.66
-1.40	-24.18	-24.31	-23.90	-24.33	-24.33	-22.51	-22.35	-22.50	-22.65	-22.84	-22.93	-20.28
-1.30	-21.14	-21.29	-20.88	-21.31	-21.31	-19.45	-19.30	-19.45	-19.60	-19.78	-19.88	-17.13
-1.20	-18.37	-18.44	-18.23	-18.66	-18.77	-16.84	-17.00	-17.09	-17.30	-17.49	-17.58	-14.35
-1.10	-15.68	-15.39	-15.70	-16.13	-16.41	-14.11	-14.54	-14.99	-15.24	-15.42	-15.52	-12.00
-1.00	-13.14	-12.29	-13.38	-13.81	-14.30	-11.35	-11.99	-13.15	-13.39	-13.58	-13.68	-10.13
-0.90	-11.17	-10.00	-11.55	-11.98	-12.81	-9.37	-11.30	-11.90	-12.34	-12.53	-12.62	-8.82
-0.80	-9.58	-8.52	-10.37	-10.80	-11.80	-8.13	-10.77	-10.92	-11.46	-11.65	-11.74	-8.15
-0.70	-8.54	-7.89	-9.88	-10.31	-11.31	-7.65	-10.00	-10.15	-10.60	-10.79	-10.88	-8.03
-0.60	-8.54	-7.89	-9.37	-9.79	-10.58	-8.07	-9.08	-9.23	-9.67	-9.86	-9.95	-8.66
-0.50	-9.24	-8.59	-8.88	-9.31	-9.31	-9.65	-8.40	-8.55	-8.69	-8.88	-8.97	-10.63
-0.40	-10.42	-11.34	-8.87	-8.80	-8.40	-12.30	-8.87	-8.82	-8.88	-9.07	-9.16	-13.38
-0.30	-11.76	-13.72	-9.92	-9.83	-9.32	-14.67	-10.73	-10.47	-10.21	-10.19	-10.29	-16.06
-0.20	-13.28	-15.88	-12.18	-11.40	-10.78	-16.86	-13.01	-12.38	-11.87	-11.61	-11.68	-18.37
-0.10	-14.85	-18.07	-14.30	-13.25	-12.53	-19.28	-15.35	-14.36	-13.58	-13.20	-13.08	-20.89
0.0	-16.44	-20.30	-16.41	-15.13	-14.31	-21.75	-17.71	-16.36	-15.30	-14.78	-14.47	-23.43
0.10	-18.04	-22.59	-18.56	-16.95	-16.01	-24.18	-20.08	-18.35	-16.98	-16.29	-15.86	-25.90
0.20	-19.66	-24.90	-20.73	-18.77	-17.68	-26.62	-22.45	-20.34	-18.66	-17.78	-17.23	-28.35
0.30	-21.27	-27.23	-22.90	-20.58	-19.34	-29.06	-24.83	-22.34	-20.33	-19.25	-18.60	-30.79
0.40	-22.89	-29.55	-25.07	-22.42	-21.01	-31.49	-27.20	-24.33	-22.01	-20.73	-19.99	-33.23
0.50	-24.52	-31.84	-27.23	-24.28	-22.70	-33.90	-29.56	-26.32	-23.69	-22.23	-21.40	-35.70
0.60	-26.14	-34.08	-29.37	-26.18	-24.42	-36.30	-31.90	-28.31	-25.37	-23.75	-22.84	-38.20
0.70	-27.77	-36.31	-31.51	-28.11	-26.14	-38.68	-34.24	-30.30	-27.05	-25.28	-24.30	-40.70
0.80	-29.41	-38.53	-33.65	-30.05	-27.87	-41.06	-36.56	-32.29	-28.73	-26.82	-25.77	-43.21
0.90	-31.03	-40.76	-35.80	-31.97	-29.59	-43.45	-38.89	-34.28	-30.41	-28.35	-27.23	-45.73
1.00	-32.64	-43.02	-37.95	-33.85	-31.31	-45.85	-41.23	-36.28	-32.10	-29.88	-28.68	-48.23
1.10	-34.24	-45.31	-40.11	-35.69	-33.02	-48.26	-43.56	-38.27	-33.80	-31.40	-30.10	-50.74
1.20	-35.84	-47.61	-42.28	-37.50	-34.73	-50.69	-45.90	-40.27	-35.49	-32.92	-31.51	-53.24
1.30	-37.42	-49.92	-44.44	-39.28	-36.43	-53.12	-48.23	-42.27	-37.19	-34.44	-32.92	-55.74
1.40	-39.00	-52.24	-46.61	-41.04	-38.13	-55.55	-50.57	-44.28	-38.89	-35.96	-34.31	-58.24
1.50	-40.58	-54.58	-48.79	-42.77	-39.82	-58.00	-52.90	-46.28	-40.60	-37.47	-35.70	-60.74
1.60	-42.14	-56.93	-50.97	-44.48	-41.51	-60.45	-55.24	-48.29	-42.31	-38.98	-37.08	-63.24
(T_j/T_o)	1.00	2.00	2.00	2.00	2.00	2.50	2.50	2.50	2.50	2.50	2.50	3.00
$\log_{10}(V_j/a_o)$	$\leq$ 0.400	$\leq$ 0.100	0.125	0.150	0.175	$\leq$ 0.100	0.125	0.150	0.175	0.200	0.225	$\leq$ 0.100

SAE ARP876C · Click to view the full PDF of arp876c

TABLE A11

GAS TURBINE JET EXHAUST NOISE PREDICTION

θ ANGLE TO INTAKE = 160.00 DEGREES

ONE-THIRD OCTAVE-BAND SOUND PRESSURE LEVEL (SPL-OASPL) DB

$\log_{10}(fD_j/\xi V_j)$											
-1.60	-27.01	-26.93	-26.88	-26.90	-27.07	-25.49	-25.41	-25.88	-25.97	-25.76	-25.77
-1.50	-23.54	-23.46	-23.41	-23.43	-23.60	-22.09	-22.01	-22.48	-22.57	-22.36	-22.37
-1.40	-20.17	-20.08	-20.03	-20.06	-20.23	-18.82	-18.74	-19.21	-19.30	-19.09	-19.11
-1.30	-17.01	-16.93	-16.88	-16.90	-17.07	-15.89	-15.81	-16.28	-16.37	-16.16	-16.17
-1.20	-14.32	-14.42	-14.69	-14.83	-15.00	-13.60	-13.59	-14.17	-14.30	-14.31	-14.32
-1.10	-12.30	-12.59	-13.12	-13.42	-13.59	-11.54	-11.60	-12.35	-12.64	-13.02	-13.04
-1.00	-11.01	-11.43	-11.98	-12.41	-12.58	-9.69	-9.81	-10.78	-11.37	-12.06	-12.07
-0.90	-10.13	-10.76	-11.46	-11.83	-12.00	-8.21	-8.40	-9.84	-10.85	-11.31	-11.33
-0.80	-9.62	-10.33	-11.08	-11.40	-11.57	-7.72	-7.93	-9.56	-10.74	-11.06	-11.07
-0.70	-9.31	-9.93	-10.59	-11.01	-11.18	-8.28	-8.40	-9.28	-10.27	-10.96	-10.97
-0.60	-8.91	-9.42	-9.87	-11.31	-11.48	-9.72	-9.74	-8.78	-9.35	-10.24	-10.25
-0.50	-9.22	-9.33	-9.39	-9.41	-9.58	-11.69	-11.42	-9.18	-9.27	-9.46	-9.47
-0.40	-10.49	-9.91	-9.37	-9.40	-9.57	-14.24	-13.68	-11.35	-10.04	-9.84	-9.86
-0.30	-12.66	-11.56	-10.90	-10.42	-10.59	-16.51	-15.95	-13.32	-11.59	-10.87	-10.88
-0.20	-15.06	-13.48	-12.57	-11.94	-12.08	-19.05	-18.22	-15.70	-13.48	-12.31	-12.32
-0.10	-17.46	-15.49	-14.38	-13.48	-13.30	-21.62	-20.47	-17.78	-15.26	-14.07	-14.04
0.0	-19.84	-17.55	-16.19	-15.01	-14.48	-24.19	-22.73	-19.80	-17.07	-15.86	-15.77
0.10	-22.20	-19.61	-17.94	-16.52	-15.75	-26.74	-25.02	-21.92	-18.98	-17.53	-17.42
0.20	-24.56	-21.68	-19.66	-18.02	-17.05	-29.28	-27.32	-24.06	-20.94	-19.15	-19.02
0.30	-26.90	-23.76	-21.37	-19.52	-18.35	-31.83	-29.63	-26.21	-22.92	-20.77	-20.62
0.40	-29.24	-25.85	-23.07	-21.03	-19.67	-34.39	-31.95	-28.36	-24.88	-22.39	-22.22
0.50	-31.58	-27.94	-24.79	-22.56	-20.98	-36.99	-34.27	-30.50	-26.82	-24.04	-23.85
0.60	-33.90	-30.04	-26.51	-24.11	-22.30	-39.62	-36.62	-32.62	-28.73	-25.73	-25.51
0.70	-36.20	-32.16	-28.23	-25.68	-23.63	-42.28	-38.97	-34.74	-30.63	-27.44	-27.19
0.80	-38.50	-34.28	-29.95	-27.25	-24.96	-44.95	-41.33	-36.86	-32.51	-29.15	-28.86
0.90	-40.81	-36.38	-31.67	-28.83	-26.28	-47.63	-43.69	-38.99	-34.40	-30.86	-30.53
1.00	-43.15	-38.47	-33.40	-30.41	-27.58	-50.29	-46.05	-41.12	-36.28	-32.56	-32.18
1.10	-45.52	-40.53	-35.13	-31.98	-28.86	-52.94	-48.40	-43.26	-38.17	-34.24	-33.81
1.20	-47.91	-42.59	-36.86	-33.56	-30.13	-55.59	-50.75	-45.40	-40.06	-35.92	-35.42
1.30	-50.30	-44.63	-38.59	-35.14	-31.38	-58.25	-58.10	-47.55	-41.94	-37.59	-37.03
1.40	-52.71	-46.66	-40.33	-36.73	-32.63	-60.89	-55.46	-49.71	-43.83	-39.25	-38.62
1.50	-55.13	-48.68	-42.06	-38.32	-33.86	-63.54	-57.81	-51.86	-45.71	-40.91	-40.21
1.60	-57.56	-50.68	-43.80	-39.90	-35.08	-66.19	-60.16	-54.03	-47.59	-42.56	-41.78
(T_j/T_o)	3.00	3.00	3.00	3.00	3.00	3.50	3.50	3.50	3.50	3.50	3.50
$\log_{10}(V_j/a_o)$	0.125	0.150	0.175	0.200	0.225	$\leq$ 0.100	0.125	0.150	0.175	0.200	0.225

SAENORM.COM : Click to view the full PDF of arp876c

TABLE A11 (CONTINUED)

VARIATION OF VELOCITY EXPONENT $m(\theta_i)$ WITH angle θ_i AND JET MACH NUMBER V_j/a_o

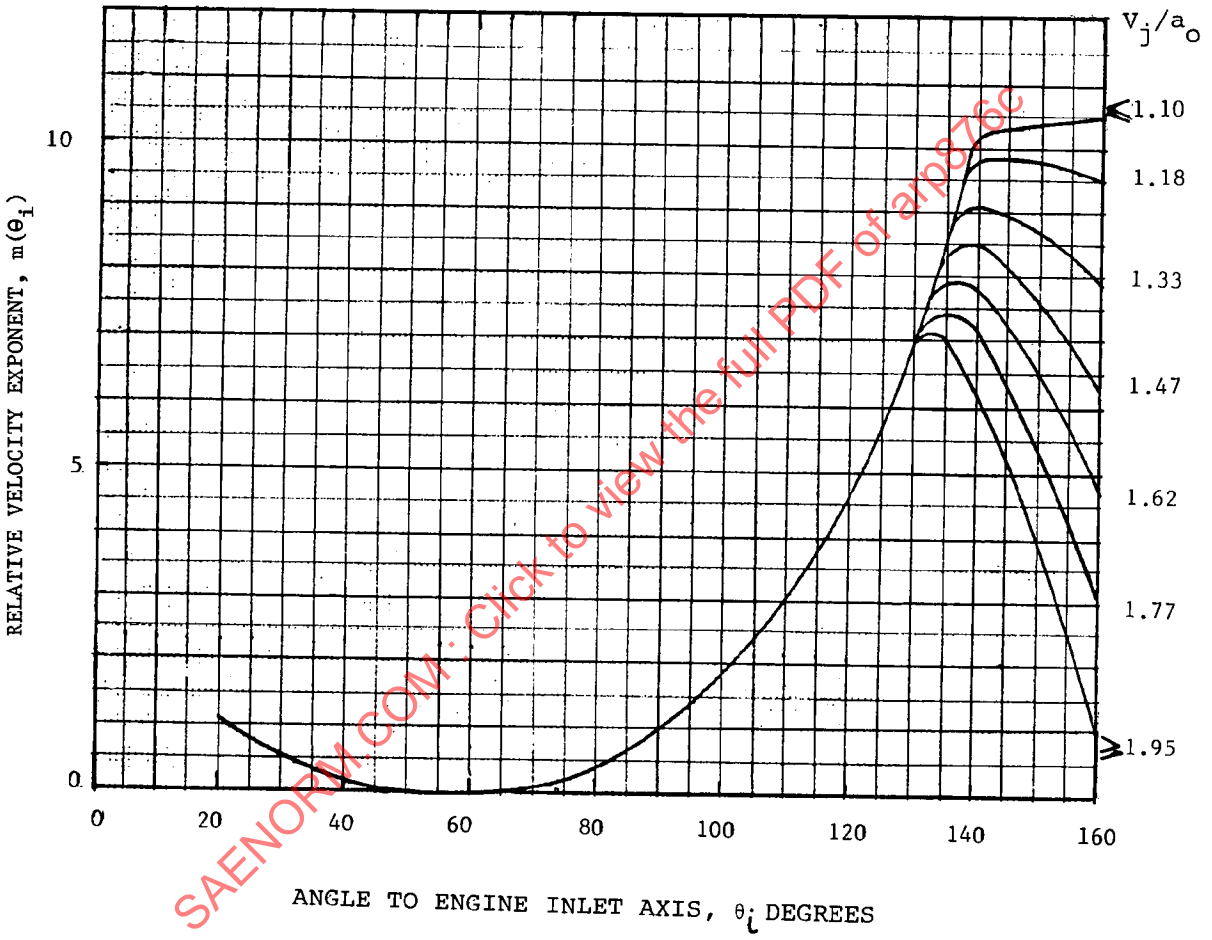

SAENORM.COM : Click to view the full PDF of arp876c

FIGURE A12

Relative velocity exponent $m(\theta_i)$

θ_i degrees	$m(\theta_i)$
20	1.1
30	0.5
40	0.2
50	0
60	0
70	0.1
80	0.4
90	1.0
100	1.9
110	3.0
120	4.7
130	7.0

$m(\theta_i)$

θ_i degrees \ V_j/a_o	≤1.10	1.18	1.33	1.47	1.62	1.77	≥1.95
140	10.2	9.8	9.1	8.5	7.8	7.2	6.3
150	10.4	9.8	8.7	7.6	6.5	5.4	4.0
160	10.5	9.5	7.9	6.3	4.7	3.1	1.0

TABLE A12

SAENORM.COM : Click to view the full PDF of arp876c

Estimated range of uncertainty associated with calculated values of ΔOASPL (θ_i) for various jet velocity ratios and uncertainty in m (θ_i).

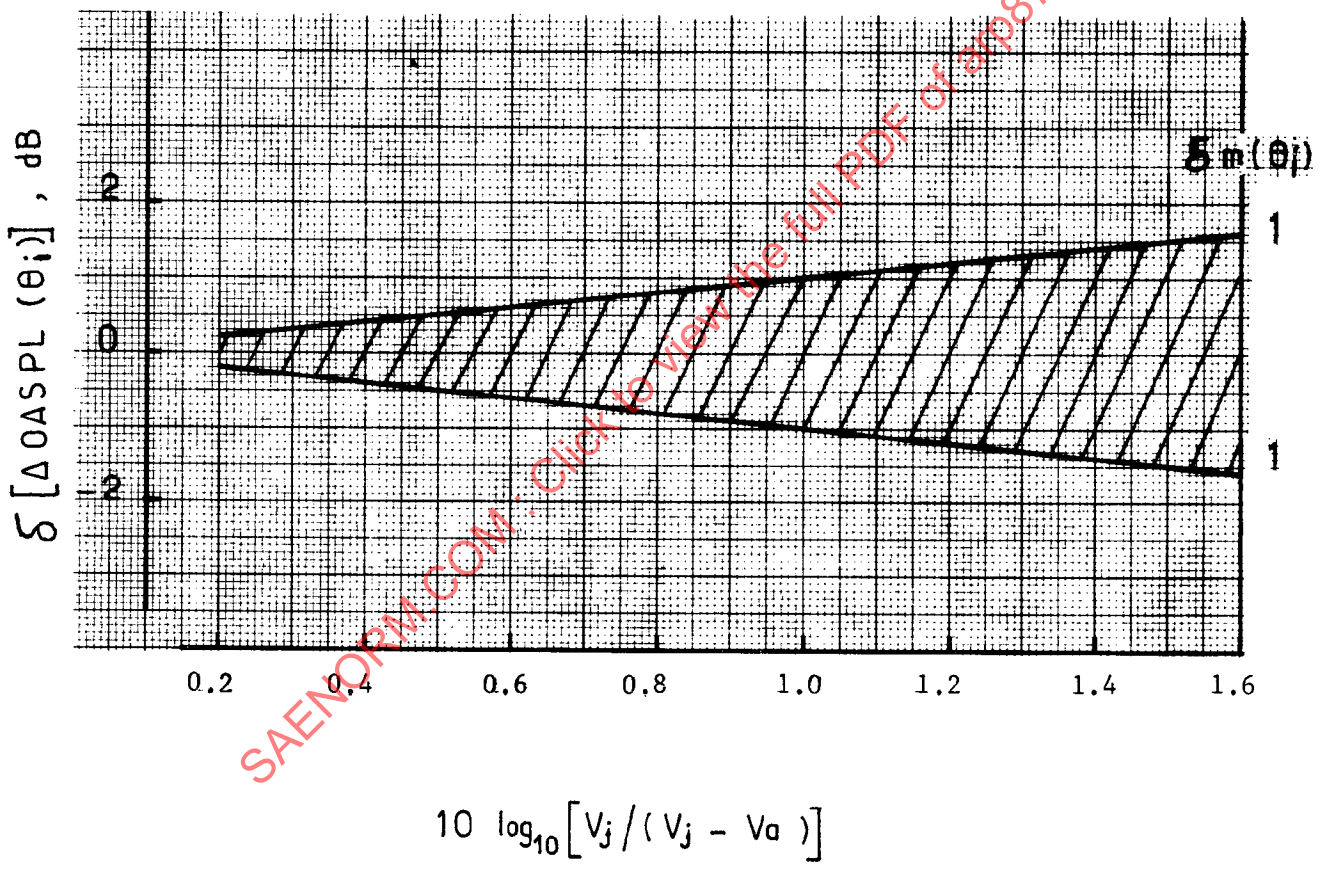

SAENORM.COM : Click to view the full PDF of arp876c

FIGURE A13

APPENDIX B

DATE OF COMPILATION
March 1980

6. PREDICTION OF SINGLE STREAM SHOCK-ASSOCIATED NOISE FROM CONVERGENT NOZZLES AT SUPERCRITICAL CONDITIONS

6.1 Static Conditions: An incorrectly expanded supersonic jet contains shock waves which interact with jet turbulence to produce a source of noise in addition to that due to the turbulent mixing process. While shock-associated noise may be reduced by attention to nozzle design, this source of noise is always present with a circular convergent nozzle. Allied to the theoretical approach of Ref. 1, definitive model and full scale experimental work (Refs. 2 and 3) has provided the following procedure for estimating the broadband shock-associated noise content. Taken together with the mixing noise prediction procedure of Appendix A, this enables the prediction of total noise from the shock-containing under-expanded jet to be executed. The method provides for the estimation of the one-third octave band sound pressure levels, which may be combined with the sound pressure levels obtained from Appendix A by adding the squared sound pressures.

Shock waves in a choked jet are responsible for a source of broadband noise which is a function of pressure ratio and nozzle diameter. The method of estimation relies upon the derivation of the one-third octave band sound pressure level at any angle from the jet axis θ_j and frequency f from the formula:

$$SPL(r,\theta_j,f) = 10\log_{10}\left(1 + [4/(Nb)]\sum_{i=1}^{N-1}\left\{[C_1(\sigma)]^{i^2}\sum_{s=0}^{N-(i+1)}[1/(\sigma q_{is})]\right.\right.$$
$$\left.\left.\times[\cos(\sigma q_{is})][\sin(b\sigma q_{is}/2)]\right\}\right)$$
$$+ 10\log_{10}[(D_j/r)^2\beta^n] + 10\log_{10}(b\sigma) + H_0(\sigma) + 148.8 \qquad (B1)$$

where

$$q_{is} = [1.7i/(V_j/a)](1 - 0.06\{s + [(i+1)/2]\})(1 - [0.7(V_j/a)\cos\theta_j]) \qquad (B2)$$

Note 1: Symbols in Section 4 apply and,

$H_0(\sigma)$ = group source strength spectrum, dB
$C_1(\sigma)$ = correlation coefficient spectrum
} master spectra given in Fig. B1 and Table B1

N = 8 (number of shocks)

b = 0.2316 (for one-third-octave-band proportional bandwidth)

SAENORM.COM : Click to view the full PDF of arp876c

Note 1 (Cont'd):

ω_c = $2\pi f$

σ = dimensionless frequency parameter = $\omega_c L/a_o$

β = pressure ratio parameter = $(M_j^2 - 1)^{1/2}$

n = exponent of pressure ratio parameter β

L = $1.1\ \beta\ D_j$, metres

M_j = fully-expanded jet Mach number

Note 2: Equation (B1) requires two master spectra as input for the prediction. These two master spectra, $H_o(\sigma)$ and $C_1(\sigma)$, are presented in Fig. B1 and the values are also tabulated for convenience in Table B1. The $C_1(\sigma)$ spectrum can be used for heated as well as unheated jet conditions. The $H_o(\sigma)$ spectrum shown here should be used for heated jets only. A heated jet is defined here as a jet having total temperature ratio greater than 1.1. For prediction at unheated conditions, the $H_o(\sigma)$ spectrum presented here should be reduced in level by 2 dB at all values of σ.

Note 3: Moreover, for the heated and unheated cases, the exponent n of the pressure ratio parameter β takes the following values:

$\beta \leq 1.0$, heated and unheated jets: n = 4

$\beta > 1.0$, heated jet: n = 2

$\beta > 1.0$, unheated jet: n = 1

Overall Sound Pressure Level Prediction

It is recommended that the wideband or overall sound pressure levels for shock-associated noise should strictly be predicted by adding the squared pressures from individual one-third octave SPL's. However, an approximate prediction of OASPL can also be obtained by using the following empirical relationships (which are independent of angle θ_j):

(a) Heated jet, $\beta \leq 1.0$:

$$\text{OASPL (dB)} = 157.5 - 20 \log_{10} (r/D_j) + 40 \log_{10} \beta \qquad (B3)$$

(b) Heated jet, $\beta > 1.0$:

$$\text{OASPL (dB)} = 157.5 - 20 \log_{10} (r/D_j) + 20 \log_{10} \beta \qquad (B4)$$

SAENORM.COM : Click to view the full PDF of arp876c

Overall Sound Pressure Level Prediction (Cont'd.)

(c) Unheated jet, $\beta \leq 1.0$:

$$OASPL\ (dB) = 155.5 - 20 \log_{10} (r/D_j) + 40 \log_{10} \beta \qquad (B5)$$

(d) Unheated jet, $\beta > 1.0$:

$$OASPL\ (dB) = 155.5 - 20 \log_{10} (r/D_j) + 10 \log_{10} \beta \qquad (B6)$$

Angular Range of Application

For unheated jets the method is accurate for $\theta_j \geq 50°$. For smaller angles detailed analysis indicates that some over-prediction may occur. However, at those angles the shock-cell noise contribution is small and prediction may be based on the mixing noise contribution alone.

For heated jets (total temperature ratios greater than approximately 1.1) the present prediction method can be applied for all $\theta_j > 30°$. The over prediction mentioned above is unimportant (and uncheckable) for the majority of rear arc angles due to the complete dominance of the contribution of jet-mixing noise.

6.2 Flight Conditions: It is widely accepted that the effect of forward speed on a source (such as the shock-cell component), which is effectively moving at the same speed as the aircraft, is affected by a 4th-power Doppler amplification factor.

To translate the spectrum levels or overall sound pressure level obtained in Section 6.1 to flight conditions, a 4th-power amplification factor should be applied as follows:

$$SPL(flight) = SPL(static) - 40 \log_{10}(1 - M_a \cos \phi) \qquad (B7)$$

where M_a = aircraft Mach number

$\phi = \theta_i -$

θ_i = angle to engine intake axis, or $(180 - \phi_j)$ where intake and jet axes are dissimilar

= angle between airplane flight path and engine thrust axis

6.3 Parties Contributing to Compilation of Appendix B:

General Electric Company, USA
Lockheed-Georgia Company, USA
Rolls-Royce Limited, United Kingdom
SNECMA, France
The University of Southampton, United Kingdom

SAENORM.COM : Click to view the full PDF of arp876c

6.4 References:

1. Harper-Bourne, M. and Fisher, M. J. — The Noise from Shock Waves in Supersonic Jets. AGARD Proceedings CP-131, September 1973.

2. Tanna, H. K. — An Experimental Study of Jet Noise, Part II: Shock Associated Noise. Journal of Sound and Vibration, Vol. 50, No. 3, 1977.

3. Chapter 4 (Shock-Associated Noise) of Technical Report AFAPL-TR-78-85. (The Generation, Radiation and Prediction of Supersonic Jet Noise - Vol. I). Prepared by Lockheed-Georgia Company, October 1978.

SAENORM.COM : Click to view the full PDF of arp876c

MASTER SPECTRA $H_0(\sigma)$ AND $C_1(\sigma)$

$\sigma = \omega_c L/a$	$H_0(\sigma)$, dB	$C_1(\sigma)$
0.2	-33.2	0.70
0.3	-27.6	0.71
0.4	-23.7	0.71
0.7	-16.1	0.72
1.0	-11.5	0.73
1.5	-6.5	0.74
2.0	-3.5	0.74
3.0	-0.7	0.71
3.5	-0.1	0.69
4.0	0.0	0.67
4.5	-0.1	0.64
5.0	-0.4	0.62
6.0	-1.3	0.58
7.0	-2.5	0.54
8.0	-3.5	0.50
10.0	-5.5	0.45
20.0	-11.8	0.28
40.0	-18.7	0.12
68.0	-23.8	0.02
70.0	-24.0	0.02

TABLE B1

SAENORM.COM : Click to view the full PDF of arp876c

MASTER SPECTRA FOR SHOCK-ASSOCIATED NOISE PREDICTION

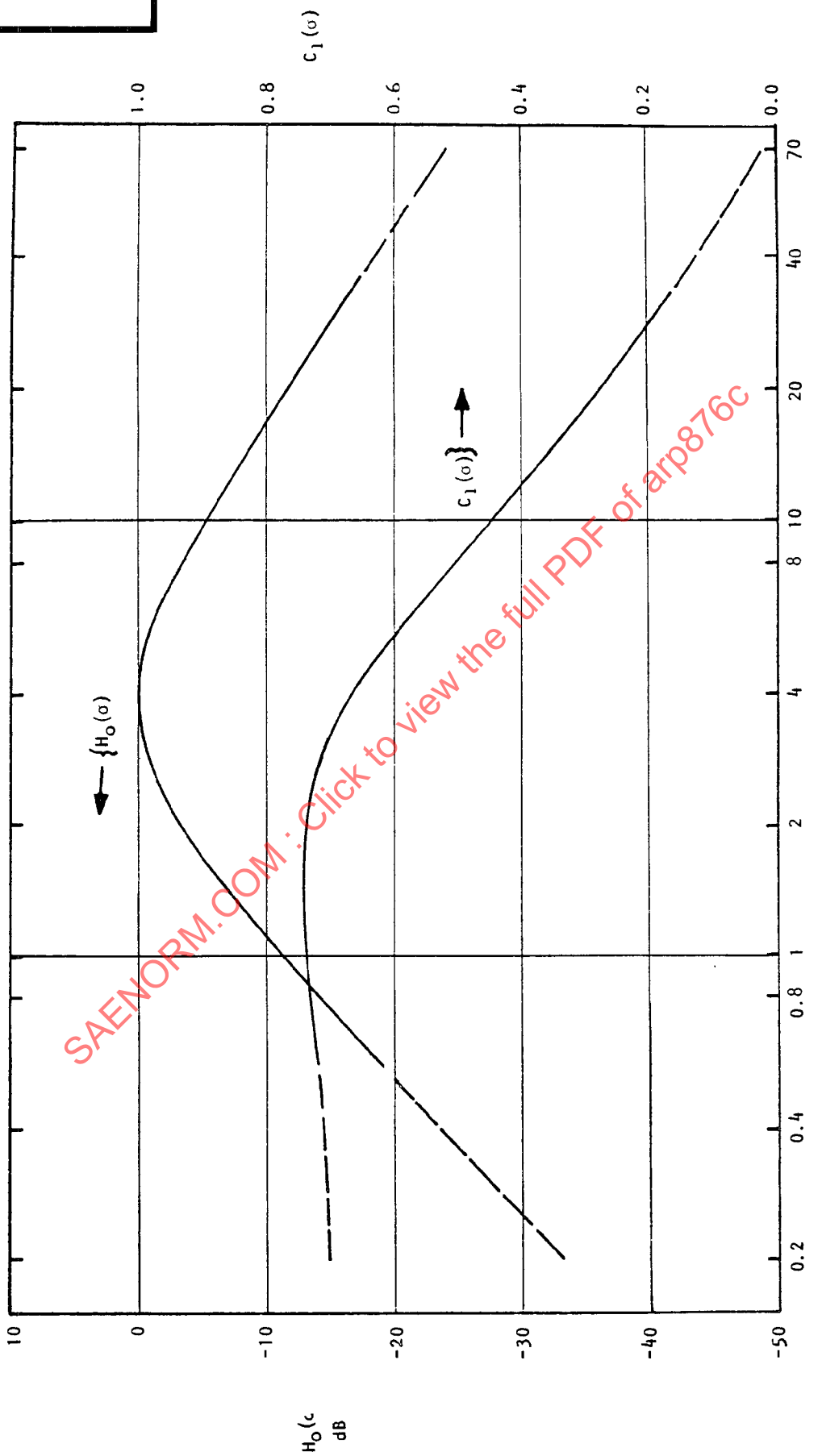

FIGURE B1

SAENORM.COM : Click to view the full PDF of arp876c

APPENDIX D

DATE OF COMPILATION
February 1980

8. PREDICTION OF NOISE FROM CONVENTIONAL COMBUSTORS INSTALLED IN GAS TURBINE ENGINES

8.1 Static Conditions: The advent of the modern high-bypass-ratio turbofan engine incorporating quiet fan technology has focused attention on internally generated core engine noise. The inherent low jet noise floor due to reduced mass efflux velocity and shielding by the fan stream has revealed low frequency noise emanating from within the core nozzle. This has variously been termed as Core Noise, Tailpipe Noise, Internal Noise, Excess Noise, and so on. Core noise has been attributed to several different sources, but the combustor in particular has received the most attention in the form of both direct combustion noise and indirect "entropy" noise. This noise source is common also to turbojet and turboshaft engines. This appendix is concerned with prediction of combustor noise from gas turbine engines.

The best definition of combustor noise is probably provided by turboshaft engines because of negligible jet noise and absence of a fan. The initial formulation of the proposed prediction method was therefore based on turboshaft engine data. However, the final correlation utilized data from all three classes of engines and the recommended spectrum and directivity have been validated using component and model data. The combustors were of various conventional types, i.e., annular, can-type, and "coannular" or hybrid type.

The prediction procedure is outlined in Figure D-1. The overall sound power level (OAPWL) is found as a function of the combustor operating parameters and turbine temperature extraction. A power level spectrum is derived by imposing a spectrum and a directivity assigned to obtain the sound pressure level (SPL) distribution at any angle. This procedure may be implemented by using Figures D-2 and D-3. For consistent application, the basic information in Figures D-2 and D-3 is repeated in Tables D-1 and D-2.

SAENORM.COM : Click to view the full PDF of arp876c

8.1 (Continued)

The method of calculation is as follows:

Step 1 - Calculate the OAPWL using the normalized sound power correlation.

$$OAPWL = 10 \log_{10}\left[\frac{\dot{M}_3 a_0^2}{\pi_{ref}}\right] + 10 \log_{10}\left\{\left(\frac{T_4 - T_3}{T_3}\right)^2 \left(\frac{P_3}{P_0}\right)^2 \left[\frac{(T_4 - T_5)_{ref}}{T_0}\right]^{-4}\right\} - 60.5 \quad (1)$$

where $\dot{M}_3$ = combustor mass flow rate, kg/s

P_3 = combustor inlet total pressure

$(T_4 - T_3)$ = combustor total temperature rise, K

$(T_4 - T_5)_{ref}$ = reference total temperature extraction by the turbines, at maximum takeoff conditions, K

π_{ref} = reference power, 10^{-12} watts (1pW)

Subscript 0 = sea level standard condition

Temperature T_0 = 288.15 K

Pressure p_0 = 1.01325 x 10^5 Pa

Speed of Sound a_0 = 340.294 m/s

Step 2 - Use Table D-1 or Figure D-2 to define the power level spectrum. For basic prediction purposes, the peak one-third octave band in the power spectrum is assumed to be 400 Hz. However, where the method is being used with data where the peak is known to be slightly above or below 400 Hz, it is recommended that the power spectrum herein be adjusted such that its symmetrical shape is retained, but based upon the observed peak freefield value. Such an adjustment would not be expected to be more than one-third octave on either side of 400 Hz. The PWL spectrum is given by:

$$PWL(f) = OAPWL + S(f) \quad (2)$$

where S (f) is the spectrum shape factor of Table D-1 and Figure D-2.

Step 3 - The sound pressure level (SPL) at each farfield angle along an arc is found using:

$$SPL(f, \theta_i) = PWL(f) + DI(\theta_i) - 20 \log_{10} r + 10 \log_{10} (\rho a \pi_{ref} / 4\pi\, Pref^2) \quad (3)$$

SAENORM.COM : Click to view the full PDF of arp876c

8.1 (Continued)

where DI - farfield directivity index (Table D-2 and Figure D-3)

θ_j = angle from inlet, degrees (axial reference from core nozzle exit)

Pref = reference pressure (20μPa)

r = arc radius, m

and where the last term is -10.8 dB under standard condition

The values thus calculated represent an idealized free field case of a non-attenuating atmosphere and absence of effects of a ground surface. In a practical case, these SPL's must be adjusted to account for atmospheric sound absorption and for ground plane effects.

Note 1 Accuracy of Prediction

It is estimated that predictions of combustor noise overall power level (OAPWL) will be accurate within +5 dB to -3 dB, based on correlation of data of turboshaft, turbojet, and turbofan engines of five manufacturers. This accuracy is estimated for the range of 186 to 222 in the Equation 1 correlating parameter.

$$10 \log_{10} (\dot{M}_3 a_o^2/\pi_{ref}) + 20 \log_{10} \left[(T_4 - T_3)/T_3\right] + 20 \log_{10} (P_3/p_0).$$

Note 2 The directivity index is assumed to be the same for all frequencies. Some model tests have indicated a change for very low frequencies, with the peak angles shifting from 120° toward the jet axis. For full-scale engines, such changes should probably be apparent for frequencies below 200 Hz. The perceived noisiness weighting for such frequencies is so small that the error accruing from use of a single directivity for all frequencies is almost negligible for perceived noise level calculations.

8.2 Flight Conditions: It is widely accepted that the effect of forward speed on a source (such as the combustor component) which is effectively moving at the same speed as the aircraft, is affected by a 4th power "Doppler" amplification factor.

To translate the sound pressure levels obtained in Section 8.1 to flight conditions, a 4th power amplification factor should be applied as follows:

$$SPL_{(flight)} = SPL_{(static)} - 40 \log_{10} (1-M_a \cos \phi)$$

SAENORM.COM : Click to view the full PDF of arp876c

8.2 (Continued)

where M_a = aircraft flight Mach number (V_a/a_o)

ϕ = $\theta_i - \psi$

θ_i = angle to engine intake axis

ψ = total incidence (angle between aircraft flight direction and engine inlet axis)

8.3 Parties Contributing to Formulation of Appendix:

AiResearch Mfg. Company of Arizona, USA
Detroit Diesel Allison, USA
General Electric, USA
Nat'l Gas Turbine Establishment, United Kingdom
Pratt & Whitney Aircraft, USA
Rolls Royce Ltd., United Kingdom
SNECMA, France
The Boeing Company, USA

8.4 References:

FAA Report No. FAA-RD-77-4
GE Core Engine Noise Investigation Program - Low Emission Engines
R. K. Matta, G. T. Sandusky, V. L. Doyle (1977)

FAA Report No. FAA-RD-74-125
Core Engine Noise Control Program - Vol. III, Supplement 1 -
Extension of Prediction Methods
S. B. Kazin, R. K. Matta, J. J. Emmerling (1976)

SAENORM.COM : Click to view the full PDF of arp876c

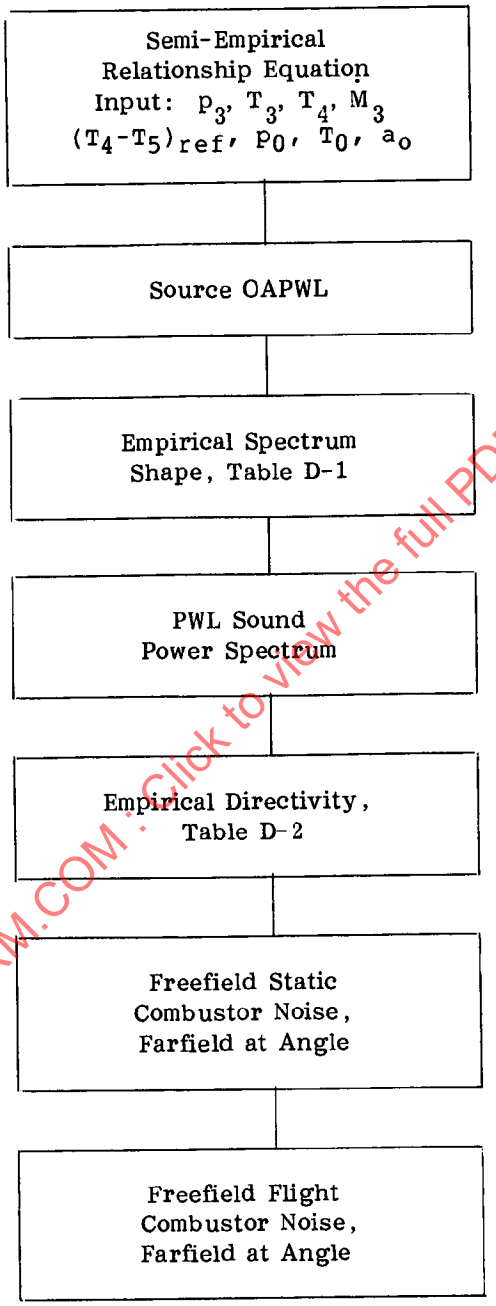

FIGURE D-1
FLOW CHART FOR COMBUSTOR NOISE PREDICTION

SAENORM.COM : Click to view the full PDF of arp876c

Table D-1

SPECTRUM SHAPE FACTOR FOR COMBUSTOR NOISE

1/3 OCTAVE BAND CENTER FREQUENCY (f), Hz	RELATIVE POWER LEVEL (PWL-OAPWL), dB
31.5	-38.7
40	-34.7
50	-31.2
63	-27.2
80	-23.2
100	-19.9
125	-17.0
160	-14.1
200	-11.7
250	- 9.7
315	- 8.2
400	- 7.2
500	- 8.2
630	- 9.7
800	-11.7
1000	-14.1
1250	-17.0
1600	-19.9
2000	-23.2
2500	-27.2
3150	-31.2
4000	-34.7
5000	-38.7
6300	-43.2
8000	-47.2
10000	-52.2

SAENORM.COM : Click to view the full PDF of arp876c

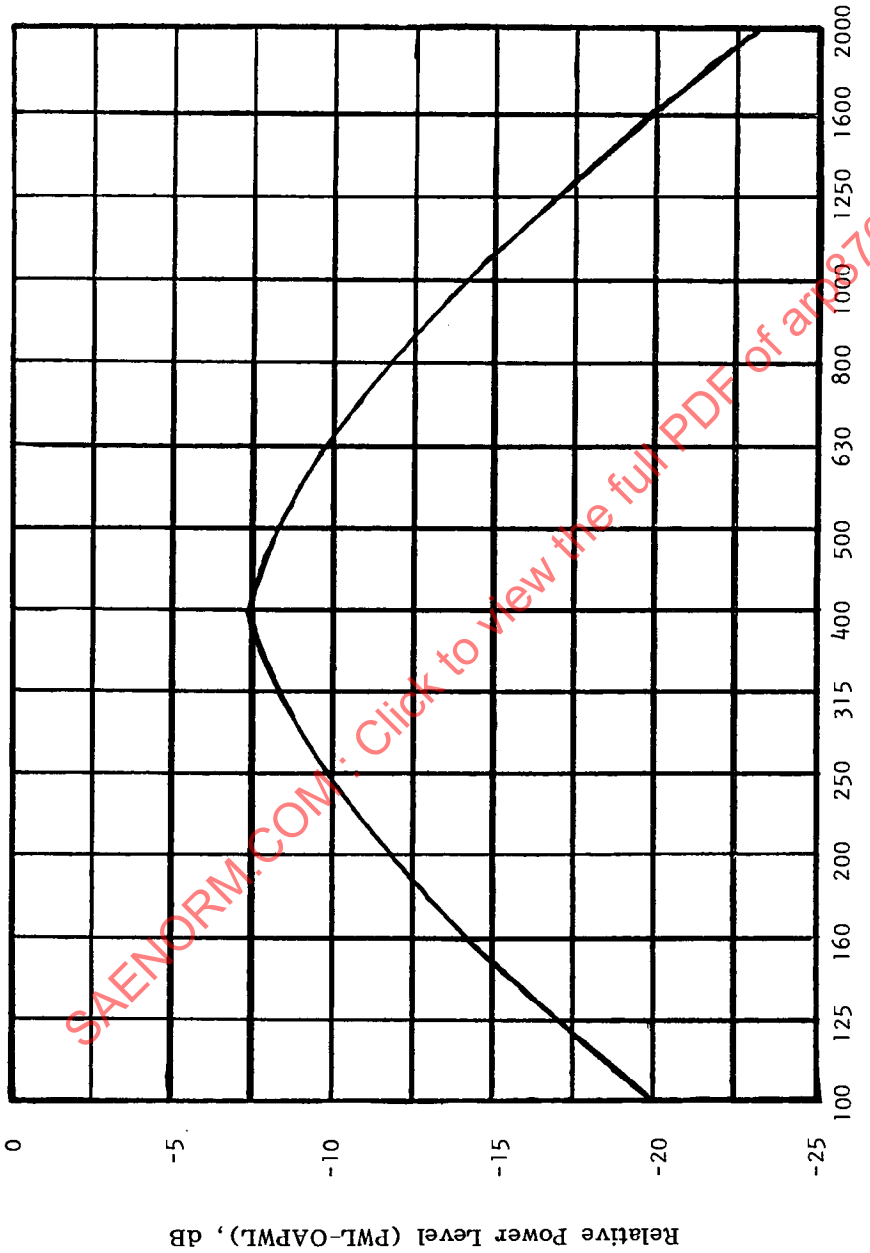

FIGURE D-2
SPECTRUM SHAPE FOR COMBUSTOR NOISE

SAENORM.COM : Click to view the full PDF of arp876c

Table D-2

FARFIELD DIRECTIVITY INDEX FOR

COMBUSTOR NOISE

Angle From Inlet* (Θ_i), degrees	Fairfield Directivity Index (DI), dB
10	-8.0
20	-7.5
30	-7.0
40	-6.5
50	-6.0
60	-5.3
70	-4.6
80	-3.9
90	-1.6
100	+0.8
110	+3.1
120	+5.0
130	+3.5
140	+1.2
150	-1.9
160	-5.1

* axial reference from core (primary) nozzle exit

SAENORM.COM : Click to view the full PDF of arp876c

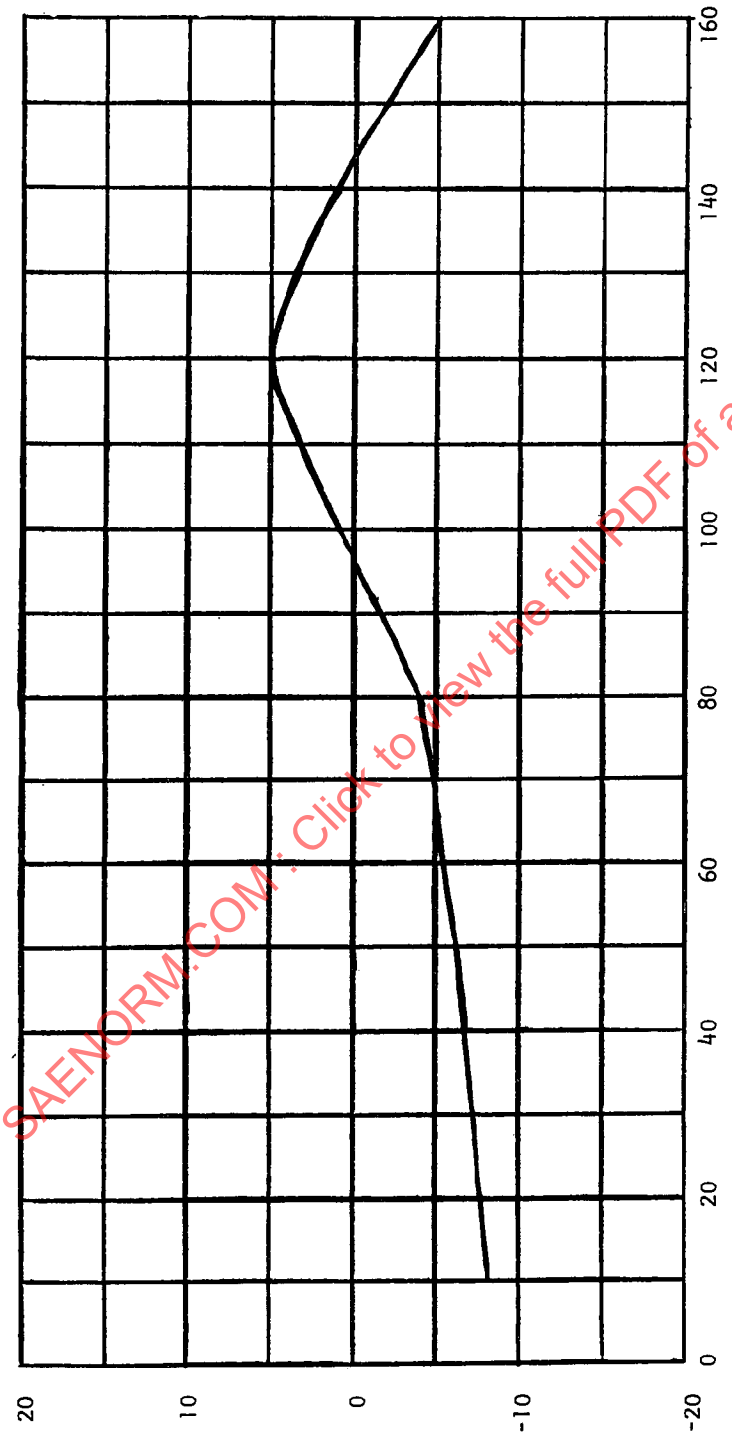

FIGURE D-3
FARFIELD DIRECTIVITY FOR COMBUSTOR NOISE

SAENORM.COM : Click to view the full PDF of arp876c

ADDENDUM TO ARP 876

A.1 BACKGROUND TO SELECTION OF PREDICTION METHODS IN ARP 876

The main body of SAE ARP 876, first published in March 1978 to replace the original and outdated SAE AIR 876 published in 1965, contains prediction methods agreed by the SAE A-21 Committee on Aircraft Noise to reflect the state of the art at the time of publication. In making its selection of a preferred method the SAE A-21 Committee has to consider:

(a) The desirability of publishing a prediction method for any particular noise-producing component of a jet engine.

(b) The amount and technical quality of the information on which the component method is based.

(c) The simplicity of correlation of available data and the level of input information required to execute a prediction.

(d) The accuracy of the final method, and

(e) Any likely foreseeable improvements brought about by new work.

Whilst Item (a) above is a prerequisite to SAE A-21 Committee activity, and Item (d) is considered in each Appendix to SAE ARP 876, items (b), (c) and (e) are the subject of protracted and exhaustive surveys and discussions in the lead-up to defining a method. In order to understand the background behind the decision to proceed with the publication of each Appendix of SAE ARP 876 it was decided to prepare this Addendum, so as to reflect the deliberations of the Gas Turbine Propulsion Subcommittee of the SAE A-21 Committee, and to reference all available information considered. It is compiled in appendix form to echo the subject matter of the main body of SAE ARP 876, and allow for future updating.

SAENORM.COM Click to view the full PDF of arp876c

A.2 HISTORY OF THE PREPARATION OF THE APPENDICES TO SAE ARP 876

In October 1970 the SAE A-21 Committee on Aircraft Noise deemed it timely to review the validity of SAE AIR 876, which was issued in 1965 as a summary correlation of jet engine exhaust noise. The need for a review was largely a function of the emergence of high bypass-ratio turbofan engines with exhaust velocities considerably lower than the range considered in SAE AIR 876, and turbojet engines for supersonic transports at the other end of the scale.

An ad hoc group was formed, and reported in 1971 that SAE AIR 876 was deficient in several significant areas over and above the question of range of jet velocities covered. Accordingly, a subcommittee was formed in 1971 which then reviewed available information over the subsequent two-year period. In 1973, the subcommittee determined that a new document should be prepared covering known sources of exhaust noise in separate prediction procedures. The topics of single and coaxial jets, shock-associated and internal noise were proposed for study. Turbomachinery noise was specifically excluded because of the proprietary nature of much of the data and because of the complication of the use of acoustically lined engine ducting for installations in high bypass-ratio turbofan engines for civil jet transport aircraft.

The depth and intensity of activity that took place in the preparation of the Appendices to SAE ARP 876 was substantial and significant. New data became available as methods were developed, and the methods were adjusted to take account of such developments. In some cases the decision to publish an Appendix at a particular date was a matter of divided opinion, since at any given time there was always a new piece of work about to produce information which might have solved immediate problems. As a result the material in the Appendices to this Addendum reflects the fact that in some instances alternative procedures were available, and that the method selected for inclusion in SAE ARP 876 was, frequently, a matter of consensus rather than unanimous agreement.

SAENORM.COM : Click to view the full PDF of arp876c

ARP 876 ADDENDUM

APPENDIX A

BACKGROUND TO PREDICTION OF SINGLE STREAM JET MIXING NOISE FROM SHOCK-FREE CIRCULAR NOZZLES

AA.1 INTRODUCTION:

Up to the time when the SAE A-21 Committee on Aircraft Noise decided to take a second look at its published method for predicting jet noise, SAE AIR 876 and the work of Coles[1] were the only published correlations of jet noise that permitted a prediction process to be undertaken. Those works stood the test of time up to the early 1970's when the introduction of the high bypass-ratio turbofan and the development of the supersonic transport revealed a need for the ability to predict jet mixing noise and other associated components of engine noise to a far greater degree of accuracy, both within and outside the jet velocity range thus far considered.

The initial move by the Exhaust Noise Subcommittee* was to circulate the then unpublished static engine and model correlations of Ahuja and Bushell[2] and to seek comparison with other available data. Such data as emerged, from the General Electric Company for models[3] and full scale engines [4], Lush[5], and the Societe Nationale d'Etude et de Construction de Moteurs d'Aviation (SNECMA) and the National Gas Turbine Establishment (NGTE)[6] revealed a sensible correlation of wideband sound pressure level values from tests of scale model nozzles, when normalised for jet area and density and referenced against fully expanded jet velocity. Discrepancies in the ability of the correlation procedure to collapse the test data were noted, however, at high velocities and temperatures (where it appeared that jet density was a variable rather than unique function) and in the considerable scatter in high frequency sound pressure levels.

SAENORM.COM : Click to view the full PDF of arp876c

AA.2 STATIC CORRELATION:

By 1973 it had been determined that the high frequency data scatter was probably a function of noise generated internally in some of the model rigs from which data had been acquired. This conclusion was borne out by the even greater variability of data from engines, first indicated by Smith[7] and later highlighted by Bushell[8] in the correlation of Fig. AA1. At

---

* Because of an enlargement of the scope of the subcommittee's responsibilities, the name of the subcommittee was changed in 1980 to the SAE A-21 Gas Turbine Propulsion Noise Subcommittee.

that time sources of noise other than those originating in the turbomachine were variously identified and labelled as core, tailpipe, excess or even combustor noise. Additional unpublished data from Pratt & Whitney Aircraft, The Boeing Company, Hamilton Standard and Pratt & Whitney Aircraft of Canada led to a close inspection of the quality of the rigs and facilities on which the data were acquired, with a view to eliminating those data that were expected to be contaminated by internal noise sources. In view of the multitude of noise sources in data from engines, it was decided to concentrate solely on information from high quality model facilities. In fact, by 1974 the second round of subcommittee activity led to significant new work being undertaken within The Boeing Company, the NGTE[9] and SNECMA on model jets, and an upsurge in activity on static-to-flight effects throughout industry and government aircraft noise research establishments.

By 1975, the acceptable data base had been reduced to measurements from the high quality facilities at SNECMA, NGTE, Boeing and General Electric. Additional high quality data from the Lockheed-Georgia Company were included at a later stage. The background data and substantiation of the method derived from this work in the period between 1975 and 1977 are contained in major internal reports[10,11,12,13] from Lockheed, SNECMA and Boeing.

The results of all this work were drawn together in the period from 1975 to 1977 in a comprehensive document correlating 1/3rd octave band spectral levels against jet velocity and density for varying temperatures. The document was approved by the SAE A-21 Committee and the SAE Aerospace Council for publication in 1977, and appeared as the initial version of Appendix A of ARP 876 in March 1978. The initial version of Appendix A dealt only with jet mixing noise from single stream shock-free circular nozzles under static conditions. The derivation of a transformation function to account for static-to-flight effects, discussed in the following paragraphs, was not finalised until 1980 and published in 1981.

AA.3 STATIC-TO-FLIGHT EFFECTS:

To be useful in predicting operational noise levels, any aircraft noise prediction method requires the ability to predict under inflight conditions. The questions of the changes that occur in the jet mixing structure as a result of forward motion and the resulting noise level and directivity are ones that have been a cause for concern for several years. The original prediction method of SAE AIR 876 of 1965 was directed primarily at providing an estimate of maximum "pass-by" noise level for aircraft Mach numbers below 0.35. The recommended curve from which the maximum pass-by noise level was ascertained was essentially an average of

SAENORM.COM : Click to view the full PDF of arp876c

ground based and flight test data using relative jet velocity as the correlating parameter. Small differences in spectra were indicated under static and flight conditions, but were not explained.

The first definitive relationship between static engine and aircraft flight levels was published by Bushell[14] in 1975. Bushell's relationship was based upon observations of the static and flight levels of a few aircraft powered by turbojet and turbofan engines. It was recognized at the time that the correlation thus produced was at variance both with the classical jet noise theory and with measurements made in wind tunnels, where forward motion was simulated by the tunnel flow [15,16]. The main differences were in the prediction of an amplification of engine noise in the forward quadrant under actual flight conditions, but a reduction under simulated flight conditions with models of the same quality as used in defining the basic jet noise correlation of SAE ARP 876 (see Fig. AA2).

The Bushell[8] correlation used as a basis the transformation function developed by Cocking and Bryce[16], which utilized an exponent (m) for the ratio of absolute to relative jet velocity and a Doppler amplification factor as shown in Fig. AA3. That format became the basis for initial studies by the A-21 Subcommittee in 1974. The aircraft static-to-flight effect seemed to be in good agreement with results from a whirling arm facility[17] and it was not until the appearance of the work of SNECMA[18,19] on the Bertin Aerotrain, work in the NASA Ames 40ft x 80 ft wind tunnel and other facilities, and new flight test evidence[20-29] that real debate started.

From that time to the date of publication of the static-to-flight section in Appendix A of SAE ARP 876, controversy continued over the real effects of forward motion on jet noise. Moreover, there was no ideal solution to the problem, since there was no accepted rationalization or explanation of the differing effects between observations on aircraft, engines under simulated flight conditions, and model jets under various modes of flight simulation.

Many possible reasons exist for these differing effects including contributions from airframe noise[30], the contribution from the core engine, engine/powerplant installation features[31] and the indication that the measured jet mixing noise from all but acoustically "clean" rigs is influenced by amplifications due to the presence of internal noise from the core engine[32,33,34]. All these effects are, of course, significant in the total process whereby the individual noise source components of an aircraft engine are built up to give the final measured aircraft flyover level (see Fig. AA4). On the other hand, it was recognized that, over and above the observed differences of single stream nozzles, there may be

SAENORM.COM : Click to view the full PDF of arp876c

significant differences between static-to-flight effects on straight turbojets and unmixed turbofans, where the twin streams from the fan and core engine discharge ducts will sense varying degrees of influence from forward motion. In fact, the work by Stone of NASA[24,35,36], which used a different, theoretically based, mode of transformation, may be as equally valid as the empirical approach based upon the Aerotrain data. The selection of the Aerotrain-based method of Section 5.2 of SAE ARP 876 was made largely because the NASA correlation relied heavily upon data from unmixed turbofan engines, whereas the Aerotrain utilized a straight turbojet engine only and produced an effect which was roughly midway between the changes observed on some aircraft installations and some models in tunnels. That is to say, the method of Appendix A was considered to provide a static-to-flight change which approximately averaged the differences in wideband sound pressure levels:

(a) Between those projected from measurements around stationary model nozzles to flight conditions and those projected to flight conditions from model tests with simulated forward motion, and

(b) Between those projected to flight conditions from measurements around an engine test stand and those obtained from flyover noise tests of aircraft installations having the corresponding engines.

As a matter of SAE policy, the SAE A-21 Committee on Aircraft Noise intends to pursue the question of static-to-flight effects on a continuing basis and will issue a revision to ARP 876 when convincing evidence is available.

AA.4 VALIDATION:

By 1980, the jet noise prediction methods of SAE ARP 876 had been checked and validated in two separate exercises. A validation of the prediction of mixing noise from shock-free jet flows under static conditions was carried out by the NASA Langley Research Center. The overall validity of the total prediction method was checked by Working Group E of the ICAO Committee on Aircraft Noise as part of a study of noise standards for future supersonic transport aircraft.

The study performed by the NASA Langley Research Center used information from the model-rig and engine-noise data bases contained in Refs. 37, 38 and 39. Comparisons between measured and predicted results were generated in terms of 1/3 octave band sound pressure levels at several angles. Spectral and directivity comparisons showed excellent agreement for all frequencies and angles for which data were available. Results in terms of wideband sound power level (PWL) in decibels re 1 pw are tabulated in Table AA1 along with relevant nozzle and jet parameters. The agreement between the measured and predicted sound pressure levels is confirmed by the sound power levels where the computed values were generally only

SAENORM.COM : Click to view the full PDF of arp876c

between 1 and 2dB lower than the measured values.

The study conducted by Working Group E of the ICAO Committee on Aircraft Noise used an early version of the method finally approved for publication in Appendix A of SAE ARP 876 for calculating the effect of forward motion in conjunction with drafts of Appendices B and D of SAE ARP 876 to predict shock and combustor noise, respectively. With due allowance for turbomachinery noise components, the total prediction method was shown to produce an average underprediction of 1 to 2dB for perceived noise level and effective perceived noise level[40]. The magnitude of the underprediction was consistent with the general results of the NASA Langley study of sound power levels and was considered to be caused by engine-installation effects, and possibly, airframe noise contributions, neither factor being considered by the prediction method.

By 1980, the basic jet mixing noise prediction method of Appendix A of SAE ARP 876 had been widely adopted by many industrial organizations and government agencies. It should be noted, however, that to account for the results of the two validation studies described above, many users increase the normalized wideband sound pressure levels of Fig. A2 and Table A2 of Appendix A of SAE ARP 876 by 1dB when predicting the jet mixing noise of full-scale turbojet engines.

SAENORM.COM : Click to view the full PDF of arp876c

REFERENCES

1. Coles, G.M. Estimating Jet Noise. Aeronautical Quarterly, Vol. 14 Part 1, pp 1-16, February 1963.

2. Ahuja, K.K. and Bushell, K.W. An Experimental Study of Subsonic Jet Noise and Comparison with Theory. Journal of Sound and Vibration, 30(3), pp 317-341, October 1973.

3. Nagamatsu, H.T., Sheer, Jr., R.E. and Gill, M.S. Flow and Acoustic Characteristics of Subsonic and Supersonic Jets from Convergent Nozzles. NASA Contractor Report CR-1693, December 1970.

4. (a) Kazin, S.B. and Paas, J.E. NASA Quiet Engine "A" Acoustic Test Results. NASA Contractor Report CR-121175, October 1973.
(b) Kazin, S.B. and Paas, J.E. NASA Quiet Engine "C" Acoustic Test Results. NASA Contractor Report CR-121176, April 1974.

5. Lush, P.A. Measurement of Subsonic Jet Noise and Comparison with Theory. Journal of Fluid Mechanics, Vol. 46(3), pp 477-500, April 1971.

6. Hoch, R.G., Duponchel, J.P., Cocking, B.J. and Bryce, W.D. Studies of the Influence of Density on Jet Noise. First International Symposium on Air Breathing Engines, Marseilles, France, June 1972 and Journal of Sound and Vibration, Vol. 28(4), pp 649-668, June 1973.

7. Smith, M.J.T. The Problem of Turbine Noise in the Civil Gas Turbine Aero Engine. ICAS, Paper No. 68-35, September 1968.

8. Bushell, K.W. A Survey of Low Velocity and Coaxial Jet Noise with Application to Prediction. Journal of Sound and Vibration, Vol. 17(2) pp 271-282, July 1971.

9. Cocking, B.J. The Effect of Temperature on Subsonic Jet Noise. National Gas Turbine Establishment, Internal Report No. R331, May 1974.

10. Tanna, H.K., Dean, P.D. and Burrin, R.H. The Generation and Radiation of Supersonic Jet Noise. Vol. III, Turbulent Mixing Noise Data. US Air Force Propulsion Laboratory Technical Report AFAPL-TR-76-65-Vol. III September 1976.

11. Hoch, R.G. and Duponchel, J.P. Revision de la Methode de Prevision du Bruits des Jets. SNECMA Document No. YKA 5317/75, January 1975.

12. Jeack, C.L., Cowan, S.J. and Gerend R.P. Empirical Jet Noise Prediction for Single and Dual Flow Jets and Without Suppressor Nozzles. Boeing Document No. D6-42929-1, Vol. 1, April 1976.

SAENORM.COM : Click to view the full PDF of arp876c

13. Hoch, R.G. and Duponchel, J.P. Comparaison des Spectres 1/3 d'Octave de Bruit de Jet Mesures en Chambre Sourde A17 du CEPr aux Diverses Propositions de Revision de l'ARP 876 de la SAE. SNECMA Document No. YKA 5898/76 July 1976.

14. Bushell, K.W. Measurement and Prediction of Jet Noise in Flight. AIAA Paper No. 75-461, March 1975.

15. von Glahn, U.H., Groesbeck, D. and Goddykoontz, J. Velocity Decay and Acoustic Characteristics of Various Nozzle Geometries in Forward Flight. AIAA Paper No. 73-629, July 1973.

16. Cocking, B.J. and Bryce, W.D. An Investigation of the Noise of Cold Air Jets Under Simulated Flight Conditions. National Gas Turbine Establishment, Internal Report R334, September 1974.

17. Smith, W. The Use of a Rotating Arm Facility to Study Flight Effects on Jet Noise. Proceedings of Second International Symposium on Air Breathing Engines. Sheffield University, England, March 1974.

18. Drevet, P., Duponchel, J.P. and Jacques, J.R. Effect of Flight on the Noise from a Convergent Nozzle as Observed on the Bertin Aerotrain. AIAA Paper No. 76-557, July 1976.

19. Hoch, R.G. and Berthelot, M. Use of the Bertin Aerotrain for the Investigation of Flight Effects on Aircraft Engine Exhaust Noise. AIAA Paper No. 76-534, July 1976.

20. Merriman, J.E., et al. Forward Motion and Installation Effects on Engine Noise. AIAA Paper No. 76-584, July 1976.

21. Plumblee, H.E. ed., A Study of the Effects of Forward Velocity on Turbulent Jet-Mixing Noise. NASA Contractor Report CR-2702, July 1976. (See also Tanna, H.K. and Morris, P.J. Inflight Simulation Experiments on Turbulent Jet Mixing Noise. AIAA Paper No. 76-554, July 1976.)

22. Pinker, R.A. and Bryce, W.D. The Radiation of Plane-Wave Duct Noise from a Jet Exhaust, Statically and In-Flight. AIAA Paper No. 76-581, July 1976.

23. Cocking, B.J. The Effect of Flight on Subsonic Jet Noise. AIAA Paper No. 76-555, July 1976. (See also A Prediction Method for the Effects of Flight on Subsonic Jet Noise. Journal of Sound and Vibration Vol. 53(3), pp 435-453, August 1977.)

24. Stone, J.R. Flight Effects on Exhaust Noise for Turbojet and Turbofan Engines - Comparison of Experimental Data with Prediction. NASA TM X-73552, November 1976.

SAENORM.COM : Click to view the full PDF of arp876c

25. Strout, F.G. and Atencio, A. Flight Effects on JT8D Engine Jet Noise Measured in a 40 x 80 Tunnel. Journal of Aircraft Vol. 14(8), pp 762-767, August 1977.

26. Blankenship, G.L., et al. Effects of Forward Motion on Engine Noise. NASA Contractor Report CR-134954, October 1977.

27. Brooks, J.R. Flight Noise Studies on a Turbojet Using Microphones Mounted on a 450ft Tower. AIAA Paper No. 77-1352, October 1977.

28. Way, D.J. The Simulation of Flight Effects on Jet Noise Using Co-Flowing Airstreams. AIAA Paper No. 77-1305, October 1977.

29. Low, J.K. Effects of Forward Motion on Jet and Core Noise. AIAA Paper No. 77-1330, October 1977.

30. Fink, M.R. Airframe Noise Prediction Method. FAA Contractor Report No. FAA-RD-77-29, March 1977.

31. Bryce, W.D. Experiments Concerning the Anomalous Behaviour of Aero-Engine Exhaust Noise in Flight. AIAA Paper No. 79-0648, March 1979.

32. Bechert, D. and Pfizenmeier, E. On the Amplification of Broadband Jet Noise by a Pure Tone Excitation. AIAA Paper No. 76-489, July 1976.

33. Deneuville, P. and Jacques, J.R. Jet Noise Amplification. A Practically Important Problem. AIAA Paper No. 77-1368 October 1977.

34. Moore, C.J. The Role of Shear-Layer Instability Waves in Jet Exhaust Noise. Journal of Fluid Mechanics, Vol. 80, Pt. 2, pp 321-367, April 1977.

35. Stone, J.R. An Improved Method for Predicting the Effects of Flight on Jet Mixing Noise. NASA TM 79-155, June 1979.

36. Stone, J.R. An Improved Method for Noise Generated in Flight by Circular Jets. NASA TM 81470, April 1980.

37. Goodykoontz, J.H. Experimental Study of Coaxial Nozzle Exhaust Noise, NASA TM 79090 and AIAA Paper No. 79-0631, March 1979.

38. Cocking, B.J. An Experimental Study of Coaxial Jet Noise. NGTE Report 333, May 1976.

39. Simcox, C.G. Boeing Company J-58 Engine Test Data, 1974. Special Communication to NASA, The Boeing Company, February 1978.

40. Smith, M.J.T.(Ch). Reports of Subcommittee on SST Noise Prediction Methods. Working Group E of ICAO Committee on Aircraft Noise (CAN), March-June 1978.

SAENORM.COM : Click to view the full PDF of arp876c

FIG.AA1

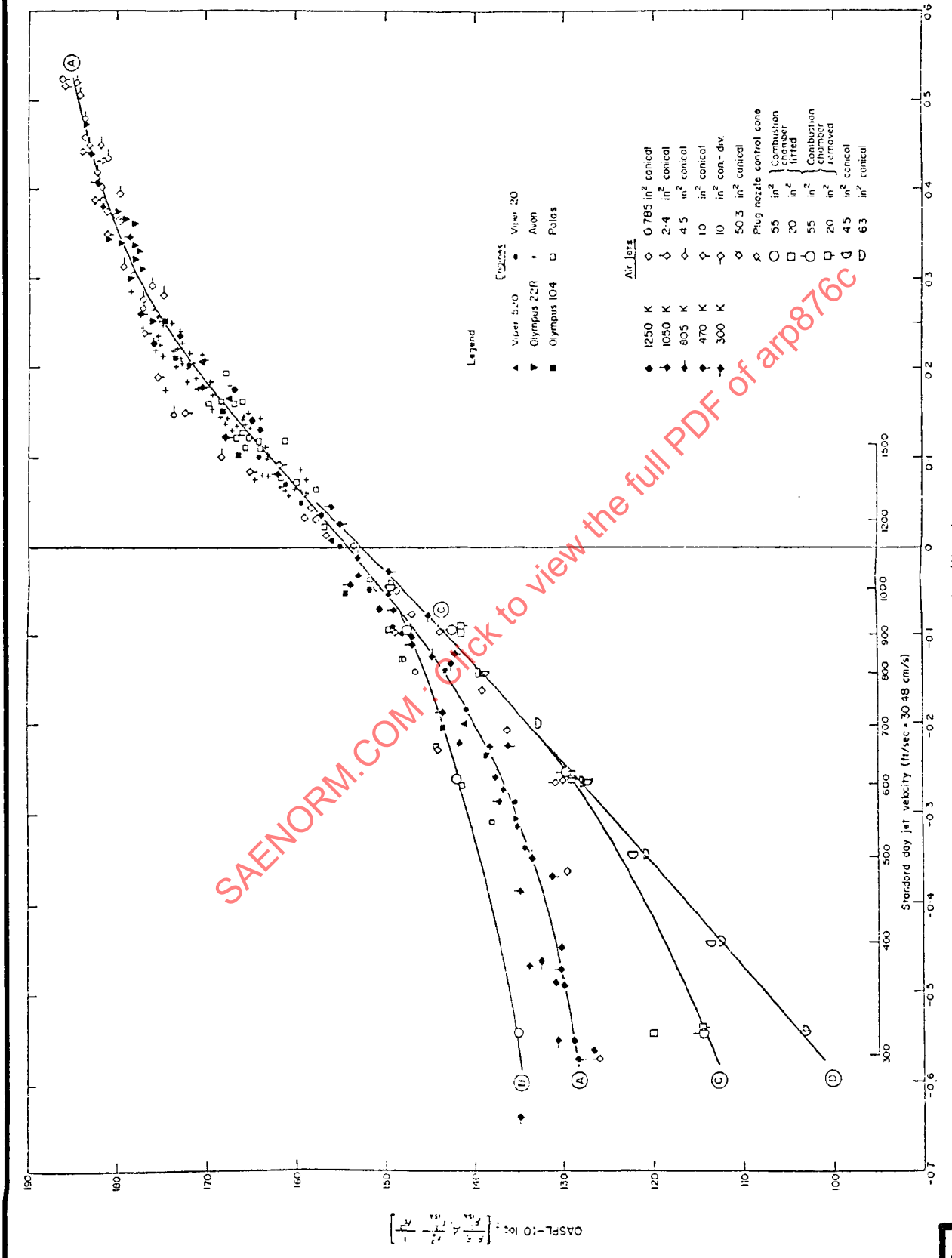

EXTRACT FROM REFERENCE 8 - EARLY JET MIXING NOISE CORRELATION

SAENORM.COM : Click to view the full PDF of arp876c

FIGURE AA2

DIFFERING FORWARD SPEED OBSERVATIONS FROM ENGINE INSTALLATIONS & MODEL JETS

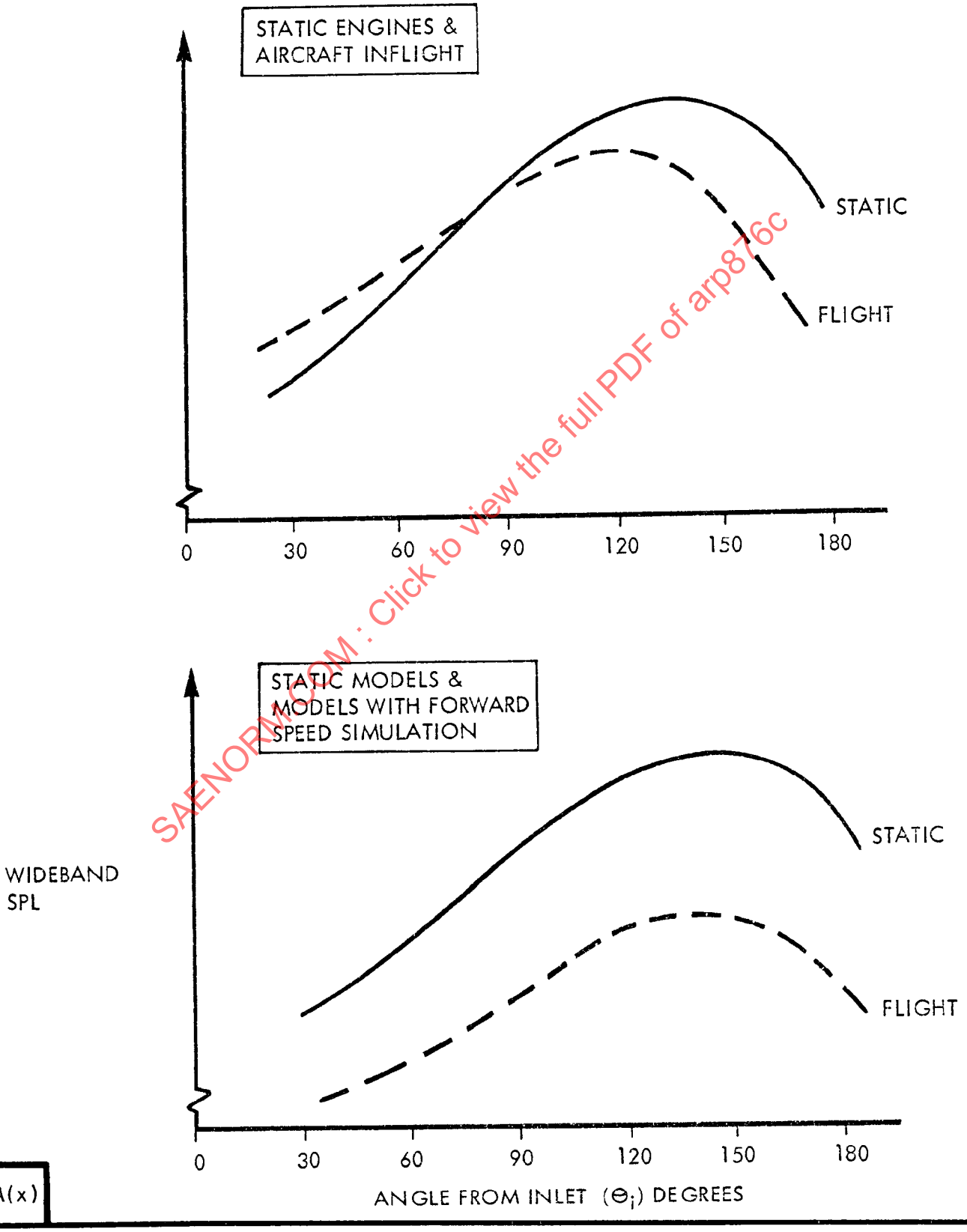

SAENORM.COM : Click to view the full PDF of arp876c